This is the accepted manuscript of the article that appeared in final form in **Journal of Sea Research** 130 : 49-72 (2017), which has been published in final form at https://doi.org/10.1016/j.seares.2017.06.002. © 2017 Elsevier under CC BY-NC-ND license (http://creativecommons.org/licenses/by-nc-nd/4.0/)

J. Rodriguez-Lazaro[a *], A. Pascual[a], I. Cacho[b], Z. Varela[a], L. D. Pena[b]

Deep-sea benthic response to rapid climatic oscillations of the last glacial cycle in the SE Bay of Biscay

[a] Department of Stratigraphy and Paleontology, University of the Basque Country (UPV/EHU). B. Sarriena, Leioa, Bizkaia. E-48940 Spain.

[b] Department of Earth and Ocean Dynamics, University of Barcelona. Martí Franquès s/n, 08028 Barcelona, Spain

*- Corresponding author: julio.rodriguez@ehu.es

Abstract

Paleoclimatic evolution of the last 140 ka (Marine Isotopic Stages MIS 1 to MIS 5) in the South Bay of Biscay has been studied by considering changes of microfossils from sediment samples of deep core PP10-17. This core was retrieved at 2882 meters water depth (mwd) in the Landas Plateau and is formed by 1792 cm of clay-silt continuously deposited sediment. A subset of 114 samples has been used for this study, yielding more than 62 thousands of specimens of foraminifers (181 benthic species, BF) and ostracods (70 spp.). Benthic response is based on main foraminifer and ostracod species by considering the oxic character and other ecological features of the assemblages. Detailed quantification of microfossils (planktonic and benthic foraminifers, ostracods) besides sedimentological and geochemical data (granulometry, magnetic susceptibility) allow us to characterize many of the climatic events registered in this core. Based on a solid chronostratigraphy by correlation with reference cores MD95-2042 (estimation of SST, sea surface T) and GICC05modelext-NGRIP 1,2 (ice core, atmospheric signal), detailed responses of benthics to cooling/warming, oxygen-content and productivity cycles have been proposed. MIS 5 was characterized by oscillations of the oceanity index (OI; 60-90); this index was higher (90-100) and stable through the MIS 4-MIS 3 intervals. We found BF species indicators of different climatic-related events. Thus, MIS 5 interglacials are evidenced by *Bulimina gibba* and *B. aculeata* while the stadials MIS 5b, d are shown by the occurrence of *Melonis pompilioides*. The Heinrich events H, when there were strong iceberg discharges into the N Atlantic Ocean, are indicated by *Globobulimina affinis*, particularly during the MIS 4 to MIS 2 interval. The beginning of MIS 4 is indicated by the entrance of new species of BF and a shift of *Cassidulina laevigata*. *Krithe* spp. and *C. laevigata* are good indicators of cold intervals of the LGM (Last Glacial Maximum, 19-23 ka) when decreased the OI. Minor cooling periods as YD (Younger Dryas, around 12-13 ka) are shown as well by a shift of *M. pompilioides,* similar to that of the MIS 5d stadial. The Holocene (11.5 ka to present) is marked by the increase of the oceanity index, disappearance of cold-water

indicators and the occurrence of *Uvigerina peregrina*. A shallow infaunal microhabitat of benthics foraminifers (*Cibicides, Cassidulina, Uvigerina*) and ostracods (*Krithe, Argilloecia*) was related with favorable bottom conditions, with oxic to slightly suboxic and relatively ventilated bottoms (high diversity and equitability of assemblages) reflecting active AMOC during many D/O interstadials. The opposite conditions were established for deep infaunal BF (*Bulimina, Globobulimina*) where the strong dysoxic bottom conditions were indicative of low ventilation produced by reduced or shutdown of the AMOC, mostly during Heinrich stadials.

Key-words: Paleoclimatology, foraminifers, ostracods, benthic response, MIS 1-MIS 5, Bay of Biscay

1. Introduction

The relationship between paleoceanography and paleoclimatology has largely been established in the comparative study of biological and bio-geochemical proxies evaluating the different responses of the sea surface and the deep sea to the atmospheric fluctuations (e.g. Cronin, 2009 and references therein; Povea et al., 2016). Though imperfect, the deep-sea benthic foraminifera oxygen isotope is the best stratigraphic reference to the study of glacial-interglacial changes (Tzedakis et al., 2009).

Taking the Atlantic Ocean as a model, the rapid alternation of warm (interstadials) and cold (stadials) intervals have been proposed as characteristic climatic oscillations during the last glacial cycle (Lisiecki and Raymo, 2005), and climatic connections with the Atlantic have been described for the Mediterranean (Cacho et al., 1999; Moreno et al., 2007). Though the cold Heinrich stadials (HS) and warm Dansgaard-Oeschger (D/O) events are reasonably known in particular to the MIS 3 (Sierro et al., 2005; Naughton et al., 2009, 2016), the details about thermal trends are yet in discussion (Long and Stoy, 2013). Rapid climate variability in N Atlantic represented by the alternation of cold and warm phases has been linked to significant changes in the strength of the AMOC (Atlantic Meridional Overturning Circulation), but particular behavior during D/O interstadials inside the Heinrich events were associated with overturning circulation rapidly transmitted across the Atlantic (Gottschalk et al., 2015).

On the other hand, the benthic response to these rapid climatic changes has been evaluated in several works for the deep N Atlantic (Baas et al., 1998; Cronin et al., 1999, 2000; Rasmussen et al., 2002; Yasuhara et al., 2008; Hoogakker et al., 2015, 2016; Grunert et al., 2015), and in the Bay of Biscay mostly relative to shelf environments during the Marine Isotope Stage MIS 3 to Holocene (Pascual et al., 2008; García et al., 2013; Martinez-Garcia et al., 2013, 2014, 2015). Recent deep benthic foraminifer distribution is well known in the area of the Bay of Biscay (Caralp et al., 1968; Pujos-Lamy, 1973, 1984). Deep benthic foraminifer distribution is influenced by

organic carbon flux, bottom currents and grain size, oxygen content and carbonate saturation of sediment (Mackensen et al., 1995; Jorissen et al., 2007). The relationship between opportunistic benthic foraminifers and primary production and oxygen content was analysed in several transects from the shelf to the bathyal Bay of Biscay by Fontanier et al. (2002, 2003, 2006) and Mojtahid et al. (2010). These authors monitored changes in the benthic microhabitat responding to the trophic conditions of the water-sediment interface following the TROX-model (TRopic conditions and OXigen concentrations) of Jorissen et al. (1995).

Several aspects of the paleoceanography of the Bay of Biscay have been previously considered. Zaragosi et al. (2001) considered surface and deep conditions in the Meriadzek Terrace. The Last Glacial Maximum (LGM) was characterized by a gradual warming with at least two pulses of the North Atlantic Drift (NAD) that finally lead to the collapse of Heinrich event H1.

Naughton et al. (2009, 2016) characterized the Heinrich events (H4 to H1) in NW Iberia comparing marine and terrestrial records. The robust chronostratigraphic framework allowed the authors revealing the complex nature of H1, describing detailed cooling/warming trends. Sanchez Goñi et al. (2013) described the MIS 5a-4 transition in N Atlantic with three cold events (C20, C19, C18; 80-70 ka BP). The thermal gradient between sea surface temperatures (SST) and air temperature (warm surface ocean in the W European marginal areas) resulted in increased input of humidity that fed the continental ice sheets in the North Atlantic.

The aim of this study is to provide with new evidence of deep-sea benthic response to rapid climate changes produced during the last glacial cycle, based on detailed new data of benthic foraminifers and ostracods completed with sedimentary analyses in a bathyal settlement in the SE Bay of Biscay.

1.1. Environmental setting

Surface circulation in the Bay of Biscay is characterized today by a general oceanic current formed by anticyclonic ENACW (Eastern North Atlantic Central Water) (Koutsikopoulos and Le Cann, 1996) and proximally by the Iberian Poleward Current (IPC), with a strong seasonal component counter-clock winter slope current (Durrieu de Madron et al. 1999; Fig. 1). In the southern area surface water circulation is mainly induced by winds and water density variations produced by freshwater runoff from French and Spanish rivers (Koutsikopoulos and Le Cann, 1996; Ferrer et al., 2009), finally producing seasonal oscillations in salinity and nutrient discharges in surface waters (Puillat et al. 2004). Inceptions of IPC current into the Bay of Biscay have been correlated to negative NAO (North Atlantic Oscillation) phases (Decastro et al. 2011).

Main water masses in the Bay of Biscay are AABW (Antarctic Bottom Water; >3000 mwd), NEADW (North East Atlantic Deep Water; 3000-1300 mwd), the high-saline MOW (Mediterranean

Outflow Water; 1300-700 mwd) and the ENACW (East North Atlantic Central Water; <700 mwd) (van Aken 2000a,b, 2001). Core of this study is located in the lower NEADW.

2. Material and methods

2.1. Core PP10-17

Data for this work come from core PP10-17, of the SARGASS oceanographic cruise, retrieved in 2010 at 2880 mwd (43º 58.91 N - 03º14.05 W; Fig. 1) in the SW Landes Plateau. Core length is 1792 cm with a lithology of silty clay continuously deposited sediment. Sedimentology processing, included granulometry and X-ray fluorescence element analyses at high resolution, has been performed at the Bordeaux I University (for details see Brocheray et al., 2014).

Samples for microfossils have been processed at the University of the Basque Country (UPV/EHU) following standard methodology. Sediment sample (1 cm max. resolution) was washed and sieved (63 μm mesh) and dried. A second separation was made, sieving with 150 μm mesh for planktonic foraminifera. Microfossils were picked using distilled water and counted: planktonic/benthic foraminifers and benthic ostracods; benthics were taxonomically determined. A subset of 114 cm samples has been used for this study, yielding more than 62 thousands of specimens of foraminifers and ostracods. Microfossil databases contain 33,110 individuals (planktonic foraminifers, PF), 27,616 individuals/181 species (benthic foraminifers, BF) and 1,299 individuals/70 species of ostracods. Taxonomic references used for foraminifers: Barker (1960), Loeblich and Tappan (1988), Holbourn et al. (2013), web-updated in Hayward et al. (2016), and for ostracods: Athersuch et al. (1989), Horne et al. (2002), Yasuhara et al. (2009).

The following quantification indices for microfossils have been used. Oceanity Index (OI; PF/PF+BF; %), a paleobathymetric estimation (Murray, 1976). Diversity of benthic assemblages has been measured with PAST 3 software (Hammer et al., 2001). Indices used for the studied core samples are: number of species (S), Shannon (H), which varies from 0 in assemblages with only one taxon, to higher values with many taxa; Equitability (J) measures the evenness of one individual to belong to a particular species. Dominance D index, takes values from 0 (even distribution in all species) to 1, when only one species dominates the assemblage, which indicates ecosystem alteration. The increasing/decreasing observed trends of these indices provide us with an estimation of stability/instability in the studied paleo-ecosystems.

3. Results

3.1. Stratigraphy and age model of core PP10-17

Stratigraphy of core PP10-17 is shown in Fig. 2. Lithologically it is composed of olive silty clay sediment with bigger grains mostly during MIS 4 interval (see Granulometry, Fig. 2A). The 114 studied samples are grouped into main units (MIS 1 to MIS 5) with dates and shifts of *Neogloboquadrina pachyderma* sin. (Nps) also indicated (Fig. 2B; data from Brocheray et al., 2014). Nps are semi-quantitatively shown by the height of rectangles, the highest representing above 95% relative of total planktonic foraminifera. Reference IMAGES core MD95-2042 from the Tagus Abyssal Plain (Cayre et al., 1999a, b; Shackleton, 2001) is used as indirect estimation of NE Atlantic Sea Surface thermal variation during the studied interval. We have drawn detailed correlations with dated samples of core PP10-17, shown by arrows in Fig. 2C. In order to compare these events with paleoclimatic signals, we use the standard core GICC05modelext-NGRIP 1,2, (version 2014-12-10, 3-point average; Rasmussen et al., 2014; Seierstad et al., 2014) as a reference for relative air temperature (T) and rapid climatic variations (Fig. 2D).

Age model for core PP10-17 is based on 38 dates (Table 1; Fig. 3A). Linear Least Squares Regression of age-depth values shows a good correlation (r= 0.96; Fig. 3B), though the best fit is performed with nonlinear logistic analysis (Fig. 3C).

3.2. Microfaunal analyses

The occurrence of Nps (*Neogloboquadrina pachyderma* sin.) in core PP10-17 (Fig. 2B) has been used as chronostratigraphic reference. Thus, core samples with Nps have been depicted in the following figures comparing with the occurrence of different assemblages of foraminifers and ostracods, as showed below.

A relative sea-level “eustatic” signal is provided by the Oceanity Index OI (Fig. 4A). MIS 5 was an oscillating interval (OI, mostly 60-90%) while the index increased and stabilized (OI, 90-100%) during MIS 4 and MIS 3 intervals, with decreasing values at the beginning of H6 and H2. There is an important and sustained decrease of the OI marking the LGM, and from H1 to recent the index increased and kept very stable around 95%.

The occurrence of benthic foraminifer species oscillates around 27 spp./sample, with clear decreases at the beginning of Heinrich events H4, 3, 2 and 1 (Fig. 4B). The presence of BF species typical of shallower areas (coastal and estuarine) (Table 2A) marks intervals (end of H6 of MIS 4, B/A of MIS 2) with important supply of detrital material to the deep studied area (Fig. 4C).

Main benthic foraminifer species occurrences in this core can be related to particular environmental benthic conditions. For example, *Cibicides wuellestorfi* is only present in noticeable percentage in the core bottom samples (Fig. 5). Since this species is characteristic of cold intervals with strong bottom circulation (see Table 3), it is possible that these samples belong to the MIS 6a stadial (see Discussion chapter).

Bulimina gibba and *B. aculeata*, species indicative of hipoxia, were very important during interstadials MIS 5a, c, e and interstadials of early MIS 3 (Fig. 5). On the other side, *Melonis barleeanus*, a cold representative, was filling the gap between the latter, in the stadial 5d, while *Melonis pompilioides* was also present in other stadials of MIS 3 and the YD (Fig. 5). *Cassidulina laevigata,* a cold water, high-nutrient content and suboxic species (see Table 3), was dominant during pre-H6 of MIS 4, the beginning of H2 and all the LGM (Fig. 6). *Globobulimina affinis*, a cold, low ventilated, low oxygen and high content OM (organic matter) water species (Table 3)*,* dominated the benthic assemblages during Heinrich stadials (HS6, HS4, HS3, HS2, HS1) and only in HS5 and LGM it was present with lower percentages (Fig. 6). *Uvigerina peregrina*, a temperate-water species, is indicative of seasonal pulses of OM to the bottom (Table 3). This species is a good marker of the Holocene in this core (Fig. 6). The milioliid genus *Pyrgo*, with the dominant species *P. murrhina*, is composed of a total of 6 species, characterizing cold and oxygenated waters in this core, with shifts in C17, H5a, H4, H3, B/A and Holocene (Fig. 6). Ostracods are regularly present in this core, but with low number of individuals and species, only increased in the MIS 2 interval (Fig. 7). The analyses of ostracod species diversity (Shannon H and Equitability J indices, Fig. 7), indicate relatively poor but stable environments for these microcrustaceans. This is supported by the low values of H (mostly <1.4) with higher H (stable environment) during MIS 5c, 5b, H3 and MIS 2. On the other side, index J is quite stable and high (>0.7) during most of core intervals, with clear decreases (instability) during H5-H4 and the LGM-H1 transition (Fig. 7).

Krithe and *Argilloecia* are dominant ostracods in the studied assemblages. Both genera are deep-sea ostracods present in all oceans (Cronin et al., 2002). *Krithe,* usually the dominant genus*,* is a cryophilic representative that has been successfully used as paleoceanographic indicator (Cronin et al., 1999, 2000; Rodriguez-Lazaro and Cronin, 1999; Dwyer et al., 2000). The record of the eight found species of *Krithe* exhibits a maximum value during the LGM with minor increases in MIS 5b and the end of H1, H2 intervals (Fig. 8A). Considering the separate record of most abundant species of *Krithe, K. trinidadensis* dominated during the LGM (Fig. 8B) and *K. aequabilis* at the H1-B/A transition (Fig. 8C). *Argilloecia acuminata*, the dominant species of the genus, is only present in MIS 5e, b, and LGM to the recent (Fig. 8D). Both *Krithe* and *Argilloecia* are shallow infaunal genera (Majoran and Agrenius, 1995), and they were restricted in the studied sea-bottom, due to the very reduced oxygen conditions. Only in intervals where dysoxic values decreased, as MIS 5b, LGM and B/A, these ostracods were present, particularly during the LGM. The genus *Krithe* is negatively affected by cold and strong dysoxic intervals and recovers during the interstadials, with suboxic (*K. trinidadensis*) or oxic (*K. aequabilis*) conditions. Thus, these species can be used as markers of benthic stressed conditions during Heinrich stadials with no deep-water formation.

3.3. Sedimentologic indices

Magnetic susceptibility shows strong shifts at HS1c and H4, and minor picks at the end of H2, HS3 and H5 and the beginning of MIS 5b (Fig. 9). Heinrich event H6 is indicated by a minor increase of susceptibility values. These important shifts of magnetic susceptibility indicate a possible entrance of fine sediments from icebergs of northern precedence (Naughton et al., 2016), and will be used in discussion chapter to characterize events H4, H2 and H1.

Calcium is a major biogenic element in this core, where it was present in high percentages during interstadials MIS 5a, c, e, and Holocene, with other minor shifts at the end of H1, H2 and H4 (Fig. 10). Sr shows a similar trend as Ca. High values of Ca/Ti are related to higher productivity of calcareous plankton during warmer periods and lower siliciclastic input from the continent (Hodell et al., 2013). Ti/Ca is used as terrigenous sediment indicator (Bassetti et al., 2016). The low values of Ti in MIS 5 are characteristic of interglacials 5a, c, e in this core (Brocheray et al., 2014). Ti and Fe, as representative of the continent inputs, exhibit anti-covariant behavior relative to Ca and Sr, with higher values during stadials and decreasing from H1 towards the recent (Fig. 10).

4. Discussion

4. 1. Bottom conditions

Stability in the benthic paleoenvironment can be evaluated by means of diversity indices of benthic foraminifer and ostracod assemblages. In the case of foraminifers (Fig. 11), Shannon H and Equitability J indices show relative stability (H>2.0, J>0.70) during most part of core record, with minima/decreasing trend during stadials HS6, 5, 4, 3, 2, and particularly during the LGM, when a strong instability is deduced by the lowest values of Shannon and Equitability indices. The transition H2 to LGM (MIS 3 to MIS 2) marks the stronger alteration of benthos, with a progressive stabilization from the late H1 to the modern deep marine ecosystems in this area. Ostracod diversity and equitability (see Fig. 7 C, D) exhibit a more irregular pattern due to the scarcity of individuals, that prevents to the strict use of these indices, but show decreases (instability) during stadials MIS 5b, d, H6, 5, 4 and the end of LGM.

The oxygen content of benthic ecosystems is evaluated in this study by considering particular benthic foraminifer assemblages, indicative of oxic, suboxic and dysoxic environments (Table 2). The evolution of these assemblages in studied core (Fig. 11) shows very low (<10%) percentages of oxic species in most units of the core, with punctuated “oxic” intervals in MIS 5e, b, H5a, just before Heinrichs H4, H3, H2, and B/A and early Holocene (Fig. 11A). Most of the assemblages are suboxic or dysoxic. Suboxic species are clearly above 50% during MIS 5d-b, early MIS 4, MIS 3 interstadials and particularly, in the LGM (Fig. 11B). On the other hand, dysoxia was evident

during MIS 5e-d transition, 5c, a, C19, C17 and all the studied Heinrich events H1 to H6 (Fig. 11C).

Dysoxia and Equitability curves of benthic foraminifers are anti-covariant along most part of the core record (see Fig. 11C, D). Since Equitability is an estimation of the stability of the benthos, this anti-covariant trend evidences important bottom instability during a good part of MIS 5 to MIS 1 interval, very likely produced by the dysoxia that affected very negatively the epi- and hipo- benthic ecosystems. Nevertheless the strongest alteration, indicated by minimum of Equitability (and Shannon index) during LGM, was actually produced by important and persistent suboxia during this interval (see Fig. 11B). These oxygenation minima are described as well during Heinrich stadials HS1, 2, 3 and Younger Dryas (YD) in deep waters of SW Iberian Margin (Grunert et al., 2015).

4.2. Paleoenvironmental characterization

Taking into account the results of different indicators used in this work, we synthesize the main environmental features of the MIS 5 to MIS 1 interval (Fig. 12).

4.2.1. MIS 5

Two bottom samples in this core contain high percentage of *C. wuellerstorfi* (see Fig. 5), a cold and high oxygen species living in waters with low organic flux from surface (see Table 3 for ecological references in the discussion chapter). On the other hand, the element patterns during this interval (Ca, Sr, minima; Ti, Fe, maxima; Fig. 10) is the same type of MIS 5d, b. These findings let us think that this interval might belong to the end of stadial MIS 6a (Fig. 12), but the lack of dates in these levels prevents to confirm this point.

MIS 5e is characterized by dominance of benthic foraminifer *Bulimina gibba* (Fig. 5), a warm water, low ventilation, low O2 and high OM content species (Table 3). BF infaunal dysoxic assemblage increases in this interval (Fig. 11), and the ostracod diversity is stable (Figs. 7, 8), indicating a relative stability of benthos. These signals could correspond with those indicated in SW Iberian Margin by Grunert et al. (2015), that the inception of interglacial MIS 5e produced reduced trophic conditions and ventilation by NEADW (North East Atlantic Deep Water) increased.

During MIS 5d *Melonis barleeanus* and *M. pompilioides* entered in this record. Both are cold, suboxic water species, with input of OM (Table 3). BF assemblages are suboxic-oxic (Fig. 11) and the species number S increased during this interval (Fig. 4). Ostracods on the contrary, suffered a fall of diversity at the beginning, due to the suboxia, and then they were present in low numbers, also during all the 5c (Figs. 7, 8). This unit registered the first sea surface cooling in this core,

though it was not very important, since there was a little signal of Nps (Fig. 2B). This cooling corresponds with the end of GS26 of GICC05modelext (Fig. 2D).

During MIS 5c there were conditions very similar to that of described to 5e (see Fig. 12).

MIS 5b exhibits similar characteristics of 5d, but with the entrance of new species as *Cassidulina laevigata*, which confirms the seasonal OM pulses indicated for 5d (Table 3). The increase of ostracod *Krithe* in these levels supports some renovation of deep waters. In this unit it is registered the second cooling (but stronger than the first one, see Nps signal in Fig. 2B).

Finally, MIS 5a contains similar BF and elements described for previous interstadials 5e, c. As we will see later, *Krithe* is negatively affected by the reduction of deep-water formation produced during the stadials. The decrease of *Krithe* in these levels of 5a occurs just before the entrance of three short cooling intervals (see Fig. 8A) and might indicate a certain restriction in benthos during this time. The three intervals of cold SST are marked by Nps shifts (the second one, at 73.9 ka, corresponds to GS20 of GICC05modelext, Fig. 2D, and C20 of Fig. 2C).

4.2.2. MIS 4

The first signal is the strong shift of *C. laevigata* (Fig. 6), opportunistic species associated with seasonal fluxes of OM. This species is characteristic of glacial stages MIS 4 and MIS 2 in the Mediterranean (Singh et al., 2015; Table 3). A comparable shift of *C. laevigata* at the beginning of H6 has been signaled in the Alboran Sea (W Mediterranean) coincident with a strong fall of $\delta^{13}C$ (Perez Martin et al., 2006). In the Portuguese margin this species occurred during glacial stages with shifts synchronic with paleoproductivity (Baas et al., 1998).

Heinrich H6 signal started with strong decrease of OI (Fig. 4) and increasing of BF dysoxics (*B. gibba* among others, see Table 3). After this, OI increased (and stabilized from the beginning of H6 onwards) and a different BF assemblage contains *G. affinis,* with increasing values during H6 (see Fig. 6). *G. affinis* is a deep bathyal species, living in high productivity, high OM waters and tolerating total dysoxia conditions (Table 3). At the same time, *Krithe* reduced drastically during these levels (Fig. 7). These findings point to reduced deep-water formation produced by AMOC weakening or even shutdown.

At the end of H6 there was the stronger shift (37% of coastal BF species; see Fig. 4, Table 2) of detrital input in these waters. Heinrich stadial H6 was an interval with deep, cold and low ventilated waters, very low oxygen content and high percentage of OM. The mentioned detrital input at the end of H6 is coincident with the HS6 (61.9 ka BP; see Fig. 4), that is, the coldest interval of this event, suggesting that they are produced during low eustatic levels, responsible of increasing erosion and transportation to the deep benthos.

The end of MIS 4 is coincident with a decrease of *G. affinis* and the entrance of *P. murrhina* (Fig. 6). The later species lives in very cold and oxic waters (Table 3) and indicates the beginning of the bottom currents reactivation in this area.

4.2.3. MIS 3

This unit started with cold, low ventilation, low oxygen and high OM waters (*G. affinis*). The entrance of *M. pompilioides* suggests colder bottom waters and flux of OM from surface productivity (Fig. 5, Fig. 6, Table 3). The occurrence of elevated percentages of *P. murrhina* (in sample 1101 cm) marks the effect of well-oxygenated waters at this point (see also Fig. 11), likely due to a relative reactivation of bottom current, defining the stadial H5a (Fig. 6), but it was not important enough to produce the recovering of benthic ostracod *Krithe* (Fig. 8).

This bottom reactivation is rapidly inactivated (*B. gibba*, warmer, dysoxic waters) during the GI (Greenland Interstadials) 13, 12, 11 (Fig. 5). The occurrence of *M. pompilioides* in GI 13, attests the effect of OM fluxes from the surface. During H5 and specially H4, *G. affinis* marks a new cooling with dysoxic waters and high OM content (Fig. 6, Fig. 11, Fig. 12). From H4 to H3 we found important variations of these indicators. The stronger shift of magnetic susceptibility is found at the end of H4 (Fig. 9), which suggests that at least fine sediments from icebergs of Northern Atlantic origin reached this location (Naughton et al., 2016). Suboxic-oxic waters dominated during this interval, except two moments with marked dysoxia (*G. affinis*; Fig. 6, Fig. 11). Shifts of *G. affinis* are described in the H4 of Portugal (Baas et al., 1998) and the H4 with IRD maxima in Bay of Biscay (Loncaric et al., 1998).

After the H4 cold and well-oxygenated waters (*C. wuellestorfi*) alternated with low oxygen (*M. pompilioides*) and warmer and high seasonal productivity waters (*U. peregrina*, Fig. 6). This interval ended just before H3 with the entrance of well-oxygenated waters (*P. murrhina*) indicative of bottom current reactivation. This oxygenation was favorable for the ostracods that responded increasing their diversity (Shannon H, Fig. 7C).

The indicators of H3 are the same as for H5 and H4 relative to *G. affinis,* suggesting a low-ventilated bottom, though the absence of *Bulimina* could indicate a not so restrictive condition. The increase of diversity of *Krithe* during H3 supports this point.

After H4 and up to end of H3 there was an increase of coastal species in the assemblages, indicative of some climatic reactivation. Cold and dysoxic waters (*G. affinis)* persisted up to the end of MIS 3, and only in two intervals where this species decreased, *C. laevigata* was indicative of well-oxygenated and intermittent flux of OM waters, as is evident in the early H2 (Fig. 6).

4.2.4. MIS 2

LGM is characterized by a strong decrease of relative sea level (OI around 70%, Fig. 4). Waters

were very strong suboxic and with high nutrient content (*C. laevigata,* Fig. 6), conditions that affected negatively the BF assemblages (equitability and diversity very low (Fig. 11), but not for the case of the ostracods, that increased their presence in these levels (Fig. 7). *C. laevigata* has been described as a common species in the Mediterranean MIS 2 (Singh et al., 2015).

At the beginning of H1 the bottom was very unfavorable for the benthics (71% of *G. affinis,* lowest number of BF species, S = 8 spp., Fig. 4); low individual numbers, species and equitability for the ostracods, Fig. 7). During H1 the oxygen recovered to oxic-suboxic conditions, the OI increased and stabilised and at the same time the percentage of *G. affinis* decreased up to 24% during this event (Fig. 6). These conditions favored the recovery of BF (Fig. 11D, E) and ostracods (Fig. 7). A comparable H1 with a shift of *G. affinis* was described in other locations of the Bay of Biscay by Loncaric et al. (1998).

The B/A (Bolling/Allerod) interval was characterized by well-oxygenated waters (*P. murrhina, Krithe aequabilis, A. acuminata* and by the arrival of shallow allochthonous specimens (Fig. 4, Fig. 6, Fig. 8). The YD was under the influence of cold, suboxic and nutrient-rich waters (*M. pompilioides*) (Fig. 5, Fig. 11).

HS1 was the most extreme of cold intervals, providing further evidence for a severe temporary reduction or even shutdown of AMOC in the North Atlantic and its export to the SW Iberian Margin (Grunert et al., 2015). Naughton et al., (2016) described Heinrich stadial 1 (HS1; 18.5-14.5 ka) as a complex interval with three phases: HS1a, (18.5-17.75 ka) extremely cold and relatively wet, SS cooling (10-8ºC), shift of NPs, shift of magnetic susceptibility; HS1b, (17.75-16.1 ka), cool and dry, NAO+(?), and HS1c, (16.1-14.6 ka) of relative sea-surface warming (2ºC), increasing of moisture and IRD shift.

We located the HS1c in core PP10-17 at the very end of H1, in sample 101 cm (16.1 ka BP, Table 1, Fig. 9), coincident with the important shift of magnetic susceptibility. We also located HS1a in sample 171 cm (18.5 ka BP, Table 1, Fig. 9), coincident with a minor shift of Nps.

Supporting these findings, SSTs of core MD95-2042 are seasonally depicted by Cayre et al. (1999a), showing important cooling (up to -12ºC) during HE1 in SW Iberian margin. The shift of transported coastal species observed in the early B/A (Fig. 4C) could have been produced by a melting pulse typical of deglaciation interval.

4.2.5. MIS 1

This interval has been relatively poorly studied, with only 5 samples. It is characterized by the occurrence of *Uvigerina peregrina* (Fig. 6), a typical species of the Holocene, indicative of well-oxygenated waters, with seasonally pulsed organic matter fluxes to the seafloor (Garcia et al., 2013) and high productivity (Table 3). The presence in these levels of *P. murrhina* confirms the mentioned quality of waters. With the inception of MIS 1, OM supply reduced and a better-

ventilated deep-water environment bathed by NEADW, was established in SW Iberian Margin (Grunert et al., 2015).

5. Conclusions

Deep-sea benthic responses to rapid paleoclimatic and paleoceanographic changes of the SE Bay of Biscay are characterized for the MIS 5 to MIS 1 interval.

Benthic foraminifer assemblages characterize the succession of oxic, suboxic and dysoxic environments, related to stadial/interstadial inceptions.

Clue-species of benthic foraminifers and ostracod assemblages evidence particular conditions of the benthos, relative to temperature, oxygen, OM and productivity of this interval. The stadials (low Ca content during MIS 5) are evidenced by variable dysoxia, which is better supported by BF species adapted to dysoxic waters, but produced stress conditions for the ostracods. These cold phases are marked by the occurrence of BF deep infaunal species *Globobulimina affinis* (Heinrich stadials, cold and very low oxygen and high OM), and by shallow infaunal species *Melonis barleeanus, M. pompilioides, Pyrgo* spp. and *Cibicides wuellestorfi* (other stadials, with higher oxygen content).

Interstadials are characterized by high Ca content (MIS 5), temperate and dysoxic waters with deep infaunal species (*Bulimina gibba,* strong eutrophic and anoxic benthos) during interstadials of MIS 5 to mid MIS 3 (GI 25 to GI 10) and by shallow infaunal (*Cassidulina laevigata,* seasonal OM fluxes to the bottom) in other interstadials from GI 9 to LGM. The ostracods, particularly *Krithe* spp., increased during interstadials, evidencing some deep-water formation.

LGM is characterized by strong suboxic waters with *Cassidulina laevigata.* MIS 1 is characterized by the occurrence of temperate species *Uvigerina peregrina.*

AMOC reduction is evidenced during cold stadials, (or shutdown, at least during H6, and maybe H1) by the indicated response of benthic foraminifer and ostracod species.

Acknowledgements

This work was supported by the Spanish Ministry of Economy and Competitiveness MINECO (OPERA project, ref. CTM2013- 48639-C2-1-R; C2-2-R). M. Cremer, EPOC, UMR 5805, Bordeaux I University is thanked for all facilities with samples of core PP10-17. L.P. acknowledges support from the Ramón y Cajal program (MINECO, Spain).

References

Altenbach, A.V., 1988. Deep sea benthic foraminifera and flux rate of organic carbon. Rev. Paléobiologie. Vol. Spec. 2, 719-720.

Altenbach, A.V., Pflaumann, U., Schiebel, R., Thies, A., Timm, S., Trauth, M., 1999. Scaling percentages and distributional patterns of benthic foraminifera with flux rates or organic carbon. J. Foraminifer. Res. 29(3), 173-185.

Athersuch, J., Home, D.J., Whittaker, J.E., 1989. Marine and Brackish Water Ostracods (superfamilies Cypridacea and Cytheracea). Synopses of the British Fauna (New Series), Vol 43, first ed. Linnean Society of London and Estuarine and Coastal Sciences Association, E.J. Brill, Leiden.

Baas, J.H., Schönfeld, J., Zahn, R., 1998. Mid-depth oxygen drawdown during Heinrich Events: Evidence from benthic foraminiferal community structure, trace fossil tiering, and benthic δ13C at the Portuguese Margin. Mar. Geol. 152(1-3), 25–55. http://dx.doi.org/10.1016/S0025-3227(98)00063-2

Barker, R.W.,1960. Taxonomic Notes on the Species Figured by H.B. Brady in his Report on the Foraminifera Dredged by H.M.S. Challenger During the Years 1873-1876. Special Publ. 9. SEPM, Tulsa.

Bassetti, M.A., Berné, S., Sicre M.A., Dennielou, B., Alonso, Y., Buscail, R., Jalali, B., Hebert, B., Menniti, C., 2016. Holocene hydrological changes in the Rhône River (NW Mediterranean) as recorded in the marine mud belt. Clim. Past Discuss. Eur. Geosci. Union (EGU), 12(7), 1539-1553. https://hal-univ-perp.archives-ouvertes.fr/hal-01357628

Bornmalm, L., Widmark, J.G.V., Malmgren, B.A., 1999. Changes in circulation and trophic levels in the Pliocene Caribbean Sea: evidence from benthic foraminifer accumulation rates. J. Foraminifer. Res. 29, 209-221.

Brocheray, S., Cremer, M., Zaragosi, S., Schmidt, S., Eynaud, F., Rossignol, L., Gillet, H., 2014. 2000 years of frequent turbidite activity in the Capbreton Canyon (Bay of Biscay). Mar. Geol. 347, 136-152. http://dx.doi.org/10.1016/j.margeo.2013.11.009

Cacho I., Grimalt, J.O., Pelejero,C., Canals, M., Sierro, J.F., Flores, J.A., Shackeleton, N., 1999. Dansgaard-Oeschger and Heinrich event imprints in Alboran Sea paleotemperatures. Paleoceanogr. 14(6), 698-705. http://dx.doi.org/10.1029/1999PA900044

Caralp, M., Klingebiel, A., Lamy, A., Latouche, C., Moyes, J., Vigneaux, M., 1968. Etude micropaleontologique, sedimentologique et geochimique de quelques carottes de sédiments récents du Golfe de Gascogne. Bull. Inst. Geol. Bassin d´Aquitaine. 5, 1-73.

Caulle, C., Koho, K. A., Mojtahid, M., Reichart, G. J., Jorissen, F. J., 2014. Live (Rose Bengal stained) foraminiferal faunas from the northern Arabian Sea: faunal succession within and below the OMZ. Biogeosciences. 11(4), 1155–1175. http://dx.doi.org/10.5194/bg-11-1155-2014

Cayre, O., Hall, M.A., Lancelot, Y., Vincent, E., 1999a. Oxygen and Carbon Isotopic Data of Core MD952042. IGBP PAGES/World Data Center-A for Paleoclimatology Data Contribution Series #1999-001. NOAA/NGDC Paleoclimatology Program, Boulder CO, USA.

Cayre, O., Lancelot, Y., Vincent, E., Hall, M.A., 1999b. Paleoceanographic reconstructions from planktonic foraminifera off the Iberian Margin: Temperature, salinity and Heinrich events. Paleoceanogr. 14(3), 384-396. http://dx.doi.org/10.1029/1998PA900027

Corliss, B.H., 1983. Distribution of Holocene deep-sea benthonic foraminifera in the southwest Indian Ocean. Deep-Sea Res. Part. A. Oceanogr. Res. Pap. 30(2), 95–117. doi:10.1016/0198-0149(83)90064-X

Cronin, T.M., DeMartino D., Dwyer, G., Rodriguez-Lazaro, J., 1999. Deep-sea ostracode species diversity: response to late Quaternary climate change. Mar. Micropaleontol. 37, 231-249 (3-4). http://dx.doi.org/10.1016/S0377-8398(99)00026-2

Cronin, T.M., Dwyer, G. Baker, P.A., Rodriguez-Lazaro, J., DeMartino, D., 2000. Orbital and suborbital variability in North Atlantic Bottom Water temperature obtained from deep-sea ostracod Mg/Ca ratios. Palaeogeogr., Palaeoclim., Palaeoecol. 162(1-2), 45-57. http://dx.doi.org/10.1016/S0031-0182(00)00104-8

Cronin, T.M., 2009. Paleoclimates: Understanding Climate Change Past and Present, first ed. Columbia University Press, New York.

De, S., Gupta, A.K., 2010. Deep-sea faunal provinces and their inferred environments in the Indian Ocean based on distribution of recent benthic foraminifera. Palaeogeogr., Palaeoclimatol., Palaeoecol. 291(3-4), 429-442. http://dx.doi.org/10.1016/j.palaeo.2010.03.012

Debenay, J.P., Konate, S., 1987. Les Foraminifères actuéls des iles de Los (Guinée). Premier inventaire, comparaison avec les microfaunes voisines. Rev. Paléobiologie. 6, 213-227.

Decastro, M., Gómez-Gesteira, M., Álvarez, I., Crespo, A.J.C., 2011. Atmospheric modes influence on Iberian Poleward Current variability. Cont. Shelf Res. 31(5), 425–432.

http://dx.doi.org/10.1016/j.csr.2010.03.004

Diz, P., Barker, S., 2016. Approaches and constraints to the reconstruction of palaeoproductivity from Cape Basin abyssal benthic foraminifera (South Atlantic). J. Micropalaeontol. 35 (2), 195-204. http://dx.doi.org/10.1144/jmpaleo2015-045

Douglas, R., Woodruff, F., 1981. Deep-sea benthic foraminífera, in: Emiliani, C. (Ed.), The Oceanic Lithosphere. The Sea. Wiley Interscience, New York, USA, Vol 7, pp. 1233-1327.

Durrieu de Madron, X., Castaing, P., Nyffeler, F., Courp, T., 1999. Slope transport of suspended particulate matter on the Aquitanian margin of the Bay of Biscay. Deep-sea Res. II: Top. Stud. Oceanogr. 46(10), 2003-2027. http://dx.doi.org/10.1016/S0967-0645(99)00053-3

Dwyer, G.S., Cronin, T.M., Baker, P.A., Rodriguez-Lazaro, J, 2000. Changes in North Atlantic deep-sea temperature during climatic fluctuations of the last 25,000 years based on ostracode Mg/Ca ratios. Geochem., Geophys., Geosystems. 1(12), 1-17. http://dx.doi.org/ 10.1029/2000GC000046

Ferrer, L., Fontán, A., Mader, J., Chust, G., González, M., Valencia, V., Uriarte, A., Collins, M.B., 2009. Low salinity plumes in the oceanic region of the Basque Country. Cont. Shelf Res. 29(8), 970-984. http://dx.doi.org/10.1016/j.csr.2008.12.014

Fontanier, C., Jorissen, F.J., Licari, L., Alexandre, A., Anschutz, P., Carbonel, P., 2002. Live benthic foraminiferal faunas from the Bay of Biscay; faunal density, composition and microhabitats. Deep-Sea Res. I: Oceanogr. Res. Pap. 49(4), 751-785. http://dx.doi.org/10.1016/S0967-0637(01)00078-4

Fontanier, C., Jorissen, F.J., Chaillou, G., David, C., Anschutz, P., Lafon, V., 2003. Seasonal and interannual variability of benthic foraminiferal faunas at 550m depth in the Bay of Biscay. Deep-Sea Res. I: Oceanogr. Res. Pap. 50(4), 457-494. http://dx.doi.org/10.1016/S0967-0637(02)00167-X

Fontanier, C., Jorissen, F.J., Chaillou, G., Anschutz, P., Grémare, A., Griveaud, C., 2005. Live foraminiferal faunas from a 2800m deep lower canyon station from the Bay of Biscay: Faunal response to focusing of refractory organic matter. Deep-Sea Res. I: Oceanogr. Res. Pap. 52(7), 1189-1227. http://dx.doi.org/10.1016/j.dsr.2005.01.006

Fontanier, C., Jorissen, F.J., Anschutz, P., Chaillou, G., 2006. Seasonal variability of foraminiferal faunas at 1000m depth in the Bay of Biscay. J. Foraminifer. Res. 36(1), 61–76. http://dx.doi.org/10.2113/36.1.61

512 Frerichs, W.E., 1970. Distribution and ecology of benthonic foraminifera in the sediments of the
513 Andaman Sea. Contrib. Cushman Found. Foraminifer. Res. 21, 123-147.

514 García, J., Mojtahid, M., Howa, H., Michel, E., 2013. Benthic and Planktic Foraminifera as
515 Indicators of Late Glacial to Holocene Paleoclimatic Changes in a Marginal Environment: An
516 Example from the Southeastern Bay of Biscay. Acta Protozool. 52, 161-180.
517 http://dx.doi.org/10.4467/16890027AP.13.0015.1112

518 Geslin, E., Heinz, P., Jorissen, F., Hemleben, C., 2004. Migratory responses of deep-sea benthic
519 foraminifera to variable oxygen conditions: laboratory investigations. Mar. Micropaleontol. 53(3-4),
520 227-243. http://dx.doi.org/10.1016/j.marmicro.2004.05.010

521 Gonzalez-Mora, B., Sierro, F.J., Flores, J.A., Berné, S., 2007. Variabilidad milenaria registrada
522 por la fauna bentónica en el Golfo de León (Mediterráneo noroccidental) entre los eventos
523 Heinrich 3 y 4. Geogaceta. 43, 115-118.

524 Gooday, A.J., 2003. Benthic foraminifera (Protista) as tools in deep-water palaeoceanography:
525 environmental influences on faunal characteristic, in Southward, A.J., Tyler, P.A., Young, C.M.,
526 Fuiman, L.A (Eds.), Advances in Marine Biology. Academic Press, London, pp. 3-90.
527 http://dx.doi.org/10.1016/S0065-2881(03)46002-1

528 Gottschalk, J., Skinner, L.C., Misra, S., Waelbroeck, C., Menviel, L., Timmermann, A., 2015.
529 Abrupt changes in the southern extent of North Atlantic Deep Water during Dansgaard–Oeschger
530 events. Nat. Geosci. 8, 950-955. http://dx.doi.org/ 10.1038/ngeo2558

531 Grunert, P., Skinner, L., Hodell, D.A., Piller, W.E., 2015. A micropalaeontological perspective on
532 export productivity, oxygenation and temperature in NE Atlantic deep-waters across Terminations I
533 and II. Glob. Planet. Change. 131, 174-191. http://dx.doi.org/10.1016/j.gloplacha.2015.06.002

534 Gudmundsson, G., 1998. Distributional limits of *Pyrgo* species at the biogeographic boundaries of
535 the Arctic and the North-Atlantic Boreal regions. J. Foraminifer. Res. 28(3), 240-256.

536 Hammer, Ø., Harper, D.A.T., Ryan, P.D., 2001. PAST: Paleontological STatistics Software
537 Package for Education and Data Analysis. Palaeontol. Electron. 4, 9.

538 Hayek, L.A.C., Wilson, B., 2013. Quantifying Assemblage Turnover and Species Contributions at
539 Ecologic Boundaries. PLoS ONE 8(10), e74999. http://dx.doi.org/10.1371/journal.pone.0074999

540 Hayward, B.W., Cedhagen, T., Kaminski, M., Gross, O., 2016. World Foraminifera Database.
541 Accessed at http://www.marinespecies.org/foraminifera on 2016-11-03

542 Hodell, D., Crowhurst, S., Skinner, L, Tzedakis, P.C., Margari, V., Channell, J.E.T., Kamenov, G.,
543 Maclachlan, S., Rothwell, G., 2013. Response of Iberian Margin sediments to orbital and
544 suborbital forcing over the past 420ka. Paleoceanogr. 28(1), 185-199.
545 http://dx.doi.org/10.1002/palo.20017

546 Holbourn, A., Henderson, A.S., Macleod, N., 2013. Atlas of benthic foraminifera, first ed. Wiley–
547 Blackwell, London.

548 Hoogakker, B.A.A., Elderfield, H., Schmiedl, G., McCave, I.N., Rickaby, R.E.M., 2015. Glacial–
549 interglacial changes in bottom-water oxygen content on the Portuguese margin. Nat. Geosci. 8,
550 40–43. http://dx.doi.org/10.1038/ngeo2317

551 Hoogakker, B.A.A., Thornalley, D.J.R., Barker, S., 2016. Millennial changes in North Atlantic
552 oxygen concentrations. Biogeosciences. 13(1), 211–221. http://dx.doi.org/10.5194/bg-13-211-
553 2016

554 Horne, D.J., Cohen, A., Martens, K., 2002. Taxonomy, morphology and biology of Quaternary and
555 living ostracoda, in: Holmes, J., Chivas, A.R. (Eds.), The Ostracoda: Applications in Quaternary
556 Research, first ed. American Geophysical Union, Washington, pp. 5-36.
557 http://dx,doi.org/10.1029/131GM02

558 Jorissen, F.J., De Stigter, H.C., Widmark, J.G.V., 1995. A conceptual model explaining benthic
559 foraminiferal microhabitats. Mar. Micropaleontol. 26(1-4), 3-15. http://dx.doi.org/10.1016/0377-
560 8398(95)00047-X

561 Jorissen, F.J., Wittling, L., Peypouquet, J.P., Rabouille, C., Relexans, J.C., 1998. Live benthic
562 foraminiferal faunas off Cape Blanc, NW Africa: community structure and microhabitats. Deep-Sea
563 Res. I: Oceanogr. Res. Pap. 45(12), 2157-2188. http://dx.doi.org/10.1016/S0967-0637(98)00056-9

564 Jorissen, F. J., Fontanier, C., Thomas, E., 2007. Paleoceanographical proxies based on deep-sea
565 benthic foraminiferal assemblage characteristics, in: Hillaire-Marcel, C., De Vernal, A. (Eds.),
566 Proxies in Late Cenozoic Paleoceanography: Pt. 2: Biological tracers and biomarkers. Elsevier,
567 Amsterdam, pp. 263-326. http://dx.doi.org/10.1016/S1572-5480(07)01012-3

568 Kaiho, K., 1994. Benthic foraminiferal dissolved-oxygen index and dissolved-oxygen levels in the
569 modern ocean. Geol. 22(8), 719-722. http://dx.doi.org/10.1130/0091-7613(1994)
570 022<0719:BFDOIA>2.3.CO;2

571 Kaiho, K., 1999. Effect of organic carbon flux and dissolved oxygen on the benthic foraminiferal
572 oxygen index (BFOI). Mar. Micropaleontol. 37(1), 67-76. http://dx.doi.org/10.1016/S0377-
573 8398(99)00008-0

574 Koutsikopoulos, C, Le Cann, B., 1996. Physical processes and hydrological structures related to
575 the Bay of Biscay anchovy. Sci. Mar. 60(2), 9-19.

576 Kuhnt, T., Schmiedl, G., Ehrmann, W., Hamann, Y., Hemleben, C., 2007. Deep-sea ecosystem
577 variability of the Aegean Sea during the past 22 kyr as revealed by Benthic Foraminifera. Mar.
578 Micropaleontol. 64, 141–162 doi:10.1016/j.marmicro.2007.04.003

579 Levy, A., Mathieu, R., Poignant, A., Rosset-Moulinier, M., Ubaldo, M.L., Lebreiro, S., 1995.
580 Foraminifères actuels de la marge continentale portuguaise-inventaire et distribution. Mem. Inst.
581 Geol. Min. Port. 32, 116 pp.

582 Lisiecki L.E., Raymo M.E., 2005. A Pliocene-Pleistocene stack of 57 globally distributed Benthic
583 $\delta^{18}O$ records. Paleoceanogr. 20(2), 1-17, http://dx.doi.org/10.1029/2004PA001071

584 Loeblich, A.R., Tappan, H., 1988. Foraminiferal Genera and Their Classification, first ed. Van
585 Nostrand Reinhold, New York.

586 Lohmann, G.P., 1978. Abyssal benthonic foraminifera as hydrographic indicators in the western
587 South Atlantic Ocean. J. Foraminifer. Res. 8(1), 6-34. http://dx.doi.org/10.2113/gsjfr.8.1.6

588 Loncaric, N., Auffret, G.A., Abrantes, F., Baas, J.H., Gaspar, L., Pujol, C., 1998. Late Quaternary
589 sedimentation patterns on the Meriadzek Terrace, Bay of Biscay (ESSCAMP 02 core: 47°N, 9°W).
590 Mar. Geol. 152(1-3), 57-73. http://dx.doi.org/10.1016/S0025-3227(98)00064-4

591 Long, J. A., Stoy, P. C., 2013. Quantifying the periodicity of Heinrich and Dansgaard–Oeschger
592 events during Marine Oxygen Isotope Stage 3. Quaternary Res. 79, 413-423.
593 http://dx.doi.org/10.1016/j.yqres.2013.02.003

594 Lutze, G.F., 1986. *Uvigerina* species of the Eastern North Atlantic, in: Van der Zwaan, G.J.,
595 Jorissen, F.J, Verhallen, P., Daniels, C. (Eds.), *Atlantic-European Oligocene to Recent Uvigerina*.
596 Utrecht Micropaleontological Bulletins, 35. University of Ultrecht, Ultrecht, pp. 21-46.

597 Mackensen, A., Grobe, H., Kuh, G., Fütterer, D.K., 1990. Benthic foraminiferal assemblages from
598 the eastern Weddell Sea between 68 and 73°S: distribution, ecology, and fossilization potential.
599 Mar. Micropaleontol. 16(3-4), 241-283. http://dx.doi.org/10.1016/0377-8398(90)90006-8

600 Mackensen, A., Schmiedl, G., Harloff, J., Giese, M., 1995. Deep-sea foraminifera in the South
601 Atlantic Ocean: ecology and assemblage generation. Micropaleontol. 41(4), 342-358.
602 http://dx.doi.org/10.2307/1485808

603 Majoran, S., Argenius, S., 1995. Preliminary observations of living *Krithe praetexta praetexta* (Sars,
604 1866), *Sarsicytheridea bradii* (Norman, 1865) and other marine ostracods in aquaria. J.
605 Micropaleontol. 14, 2, 96. http://dx.doi.org/10.1029/2003GC000595

606 Martínez- García, B., Pascual, A., Rodríguez-Lázaro, J., Bodego, A., 2013. Recent benthic
607 foraminifers of the Basque continental shelf (Bay of Biscay, Northern Spain): Oceanographic
608 implications. Cont. Shelf Res. 66, 105-122. http://dx.doi.org/10.1016/j.csr.2013.07.006

609 Martínez- García, B., Bodego, A., Mendicoa, J., Pascual, A., Rodríguez-Lázaro, J., 2014. Late
610 Quaternary (Marine Isotope Stage 3 to Recent) sedimentary evolution of the Basque shelf
611 (southern Bay of Biscay). Boreas. 43(4), 973-988. http://dx.doi.org/10.1111/bor.12079

612 Martínez- García, B., Rodríguez-Lázaro, J., Pascual, A., Mendicoa, J., 2015. The "Northern
613 guests" and other paleoclimatic ostracod proxies in the late Quaternary of the Basque Basin (S
614 Bay of Biscay) Palaeogeogr., Palaeoclimatol.,Palaeoecol. 419, 100-114.
615 http://dx.doi.org/10.1016/j.palaeo.2014.06.032

616 Mendes, L., González, R., Lobo, F., Dias, J.M.A., Martins, V., 2004. Factors influencing recent
617 benthic foraminifera distribution on the Guadiana shelf (Southwestern Iberia). Mar Micropaleontol.
618 51(1-2), 171-192. http://dx.doi.org/10.1016/j.marmicro.2003.11.001

619 Mojtahid, M., Griveaud, C., Fontanier, C., Anschutz, P., Jorissen, F.J., 2010. Live benthic
620 foraminiferal faunas along a bathymetrical transect (140-4800 m) in the Bay of Biscay (NE
621 Atlantic). Rev. Micropaleontol. 53(3), 139-162. http://dx.doi.org/10.1016/j.revmic.2010.01.002

622 Mojtahid, M., Jorissen, F.J., Garcia, J., Schiebel, R., Michel, E., Eynaud, F., Gillet, H., Cremer, M.,
623 Diz, P., Siccha, M., Howa, H., 2013. High resolution Holocene record in the southeastern Bay of
624 Biscay: Global versus regional climate signals. Palaeogeogr., Palaeoclimatol., Palaeoecol. 377,
625 28-44. http://dx.doi.org/10.1016/j.palaeo.2013.03.004

626 Moreno, A., Cacho, I., Canals, M., Grimalt, J.O., Sánchez-Goñi, M.F. Sierro, F.J., 2007.
627 Conexiones climáticas de escala milenaria entre progresos oceánicos y atmosféricos durante el
628 último ciclo glaciar: estudio multidisciplinar de un sondeo del mar de Alborán (Mediterráneo
629 occidental). Revista de la Soc. Geológica de España. 20(1-2), 31-51.

630 Murgese, D.S., De Deckker, P., 2005. The distribution of deep-sea benthic foraminifera in core
631 tops from the eastern Indian Ocean. Mar. Micropaleontol. 56(1-2), 25-49.
632 http://dx.doi.org/10.1016/j.marmicro.2005.03.005

633 Murray, J.W., 1976. A method of determining proximity of marginal seas to an ocean. Mar. Geol.
634 22(2),103-119. http://dx.doi.org/10.1016/0025-3227(76)90033-5

635 Murray, J.W., 1991. Ecology and palaeoecology of benthic foraminifera, first ed. Longman,
636 Harlow.

637 Naughton, F., Sanchez-Goñi, M.F., Kageyama, M., Bard, E., Duprat, J., Cortijo, E., Desprat, S.,
638 Malaize, B., Joli, C., Rostek, F., Turon, J.L., 2009. Wet to dry climatic trend in north western Iberia
639 within Heinrich events. Earth Planet. Sci. Lett. 284(3-4), 329-342.
640 http://dx.doi.org/10.1016/j.epsl.2009.05.001

641 Naughton, F., Sanchez-Goñi, M.F., Rodrigues, T., Salgueiro, E., Costas S., Desprat, S., Duprat,
642 J., Michel, E., Rossignol, L., Zaragosi, S., Voelker, A.H.L., Abrantes, F., 2016. Climate variability
643 across the last deglaciation in NW Iberia and its margin. Quat. Int. 414, 9-22.
644 http://dx.doi.org/10.1016/j.quaint.2015.08.073

645 Otvos, G.E., 2014. The Last Interglacial Stage: Definitions and marine highstand, North America
646 and Eurasia. Quat. Int. 383, 158-173. http://dx.doi.org/10.1016/j.quaint.2014.05.010

647 Pascual, A., Rodriguez-Lazaro, J., Martin-Rubio, M., Jouanneau, J.-M., Weber, O., 2008. A survey
648 of the benthic microfauna (foraminifera, ostracoda) on the Basque shelf, southern Bay of Biscay.
649 J. Mar. Syst. 72(1-4), 35-63. http://dx.doi.org/10.1016/j.jmarsys.2007.05.015

650 Patarroyo, G.D., Martínez, J.I., 2016. Paleoxigenación y paleoproductividad en el golfo de
651 Panamá durante el Holoceno tardío. Bol. Geolog. 38(2), 75-92.
652 http://dx.doi.org/10.18273/revbol.v38n2-2016005

653 Pérez-Martín, R., Sierro, F.J., Flores, J.A., 2006. Variaciones en las faunas de foraminíferos
654 bentónicos del Mar de Alborán durante el evento Heinrich 6. Geogaceta. 40, 223-226.

655 Povea, P., I. Cacho, A. Moreno, L. D. Pena, M. Menéndez, E. Calvo, M. Canals, R. S. Robinson,
656 F. J. Méndez, and J.-A. Flores (2016), Atmosphere-ocean linkages in the eastern equatorial
657 Pacific over the early Pleistocene, Paleoceanography. 31, 1-17.
658 http://dx.doi.org/10.1002/2015PA002883.

659 Puillat, I., Lazure, P., Jegou, A.M., Lampert, L., Miller, P.I., 2004. Hydrographical variability on the
660 French continental shelf in the Bay of Biscay, during the 1990s. Cont. Shelf Res. 24(10), 1143-
661 1163. http://dx.doi.org/10.1016/j.csr.2004.02.008

662 Pujos-Lamy, A., 1973. Repartition bathymetrique des foraminifères benthiques du Golfe de
663 Gascogne. Comparaison avec d'autres aires oceaniques. Rev. Esp. Micropaleontol. 5(2), 213-
664 234.

665 Pujos-Lamy, A., 1984. Foraminifères Benthiques et Bathymetrie: Le Cenozoique du Golfe de
666 Gascogne. Palaeogeogr. Palaeoclimatol. Palaeoecol. 48, 39-60.

667 Rai, A.K., Singh, V.B., 2012. Response of eastern Indian Ocean (ODP Site 762B) benthic
668 foraminiferal assemblages to the closure of the Indonesian seaway. Oceanologia. 54(3), 449-472.
669 http://dx.doi.org/10.5697/oc.54-3.449

670 Rasmussen, T.L., Thomsen, E., Troelstra, S.R., Kuijpers, A., Prins, M.A., 2002. Millennial-scale
671 glacial variability versus Holocene stability: changes in planktic and benthic foraminifera faunas
672 and ocean circulation in the North Atlantic during the last 60000 years. Mar. Micropaleontol. 47(1-
673 2), 143-176. http://dx.doi.org/10.1016/S0377-8398(02)00115-9

674 Rasmussen, S.O., Bigler, M., Blockley, S.P., Blunier, T., Buchardt, S.L., Clausen, H.B., Cvijanovic,
675 I, Dahl-Jensen, D., Johnsen, S.J., Fischer, H., Gkinis, V., Guillevic, M., Hoek, W.Z., Lowe, J.J.,
676 Pedro, J.B., Popp, T., Seierstad, I.K., Steffensen, J.P., Svensson, A.M., Vallelonga, P., Vinther,
677 B.M., Walker, M.J.C., Wheatley, J.J., Winstrup, M., 2014. A stratigraphic framework for abrupt
678 climatic changes during the Last Glacial period based on three synchronized Greenland ice-core
679 records: refining and extending the INTIMATE event stratigraphy. Quat. Sci. Rev. 106, 14-28.
680 http://dx.doi.org/10.1016/j.quascirev.2014.09.007

681 Rodríguez-Lazaro, J., Cronin, T.M., 1999. Quaternary glacial and deglacial Ostracoda in the
682 thermocline of the Little Bahama Bank (NW Atlantic): palaeoceanographic implications.
683 Palaeogeogr. Palaeoclimatol. Palaeoecol. 152(3-4), 339-364. http://dx.doi.org/10.1016/S0031-
684 0182(99)00048-6

685 Sánchez-Goñi, M.F., Bard, E., Landais, A., Rossignol, L., d'Errico, F., 2013. Air–sea temperature
686 decoupling in western Europe during the last interglacial–glacial transition. Nat. Geosci. 6, 837-
687 841 http://dx.doi.org/10.1038/NGEO1924

688 Seierstad, I.K., Abbott, P.M., Bigler, M., Blunier, T., Bourne, A.J., Brook, E., Buchardt,
689 S.L., Buizert, C., Clausen, H.B., Cook, E., Dahl-Jensen, D., Siwan M.
690 Davies,S.M., Guillevic,M., Johnsen,S.J., Pedersen,D.S., Popp,T.P, Rasmussen,

691 S.O., Severinghaus,J.P., Anders Svensson, A., Vinther, B.M., 2014. Consistently dated records
692 from the Greenland GRIP, GISP2 and NGRIP ice cores for the past 104 ka reveal regional
693 millennial-scale $\delta^{18}O$ gradients with possible Heinrich event imprint. Quat. Sci. Rev. 106, 29-46.
694 http://dx.doi.org/10.1016/j.quascirev.2014.10.032

695 Schnitker, D., 1979. The deep waters of the western North Atlantic during the past 24000 years,
696 and the re-iniciation of the Western Boundary Undercurrent. Mar. Micropaleontol. 4, 265-280.
697 http://dx.doi.org/10.1016/0377-8398(79)90020-3

698 Schönfeld, J., 2001. Benthic foraminifera and pore-water oxygen profiles: a reassessment of
699 species boundary conditions at the western Iberian margin. J. Foraminifer. Res. 31(2), 86-107.
700 http://dx.doi.org/10.2113/0310086

701 Shackleton, N., 2001. $\delta^{18}O$ (planktic foraminifera) of sediment core MD95-2042. PANGAEA.
702 http://dx.doi.org/10.1594/PANGAEA.58210

703 Sierro, F. J., Hodell, D. A., Curtis, J. H. , Flores, J. A., Reguera, I., Colmenero-Hidalgo, E.,
704 Bárcena, M. A., Grimalt, J. O., Cacho, I., Frigola, J., Canals, M., 2005. Impact of iceberg melting
705 on Mediterranean thermohaline circulation during Heinrich events. Paleoceanography. 20,
706 PA2019. http://dx.doi.org/10.1029/2004PA001051, 2005

707 Singh, A.D., Rai, A.K., Tiwari, M., Naidu, P.D., K. Verma, M. Chaturvedi, A. Niyogi, Pandey, D.,
708 2015. Fluctuations of Mediterranean Outflow Water circulation in the Gulf of Cadiz during MIS 5 to
709 7: Evidence from benthic foraminiferal assemblage and stable isotope records. Glob. Planet.
710 Change. 133, Pages 125-140. http://dx.doi.org/10.1016/j.gloplacha.2015.08.005

711 Tzedakis, P.C., Raynaud, C., McManus, J.F., Berger, A., Brovkin, V., Kiefer, T., 2009. Interglacial
712 diversity. Nat. Geosci. 2, 751-755. http:/dx.doi.org/10.1038/ngeo660

713 van Aken, H.M., 2000a. The hydrography of the mid-latitude northeast Atlantic Ocean I: The deep
714 water masses. Deep-Sea Res. I.: Oceanogr. Res. Pap. 47(5), 757–788.
715 http://dx.doi.org/10.1016/S0967-0637(99)00092-8

716 van Aken, H.M., 2000b The hydrography of the mid-latitude Northeast Atlantic ocean II: The
717 intermediate water masses. Deep-Sea Res. I.: Oceanogr. Res. Pap. 47(5), 789–824.
718 http://dx.doi.org/10.1016/S0967-0637(99)00112-0

719 van Aken, H.M., 2001. The hydrography of the mid-latitude Northeast Atlantic Ocean- Part III: the
720 subducted thermocline water mass. Deep-Sea Res. I.: Oceanogr. Res. Pap. 48(1), 237-267.
721 http://dx.doi.org/10.1016/S0967-0637(00)00059-5

722 Wells, P., Wells, G., Cali, J., Chiva, A.R., 1994. Response of deep-sea benthic foraminifera to Late
723 Quaternary climate changes, southeast Indian Ocean, offshore Western Australia. Mar.
724 Micropaleontol. 23(3), 185-229. http://dx.doi.org/10.1016/0377-8398(94)90013-2

725 Yasuhara, M., Cronin, T.M., deMenocal, P.B., Okahashi, H., Linsley, B.K., 2008. Abrupt climate
726 change and collapse of deep-sea ecosystems. Proc. Natl. Acad. Sci. USA, 105(5), 1556–1560.
727 http://dx.doi.org/10.1073_pnas.0705486105

728 Yasuhara, M., Okahashi, H., Cronin, T.M., 2009. Taxonomy of Quaternary deep-sea Ostracods
729 from the Western North Atlantic Ocean. Palaeontology. 52(4), 879–931.
730 http://dx.doi.org/10.1111/j.1475-4983.2009.00888.x

731 Zaragosi, S., Eynaud, F., Pujol, C., Auffret, G.A., Turon, J.L., Garlan, T., 2001. Initiation of the
732 European deglaciation as recorded in the northwestern Bay of Biscay slope environments
733 (Meriadzek Terrace and Trevelyan Escarpment): A multi-proxy approach. Earth Planet. Sci. Lett.
734 188(3-4), 493–507. http://dx.doi.org/10.1016/S0012-821X(01)00332-6

735

736

737 **Figure Captions**

738 **Figure 1**. Location of studied area with core PP10-17 and core MD95-2042.

739 **Figure 2**. Stratigraphy of core PP10-17, compared with standard marine MD95-2042 and ice
740 GICC05modelext-NGRIP cores. A-B, data from core PP10-17. A. Granulometry indicating silty
741 clay size sediment with bigger grains mostly during MIS 4 interval. B. Samples studied in core
742 PP10-17, grouped into main units. Tie-points of Heinrich stadials (HS) and Greenland
743 interstadials (GI) with dates from Table 1. Shaded (blue in web version) rectangles are shifts of the
744 cold-water planktonic foraminifer *Neogloboquadrina pachyderma* sin. (Nps), the height of
745 rectangle is the approximate percentage of Nps (highest is >90%), indicative of the sea- surface
746 cold intensity. Dates (see Table1) and events are indicated. H1 to H6, Heinrich events. GI, 1 to 25,
747 from core GICC05modelext-NGRIP. C. Reference core MD95-2042 (Cayre et al., 1999a;
748 Shackleton, 2001) is used as comparative model for SST during the studied interval. Detailed
749 correlations with dated samples from core PP10-17 are shown by arrows. D. Core
750 GICC05modelext-NGRIP 1,2, version 2014-12-10, 3-point average (Rasmussen et al., 2014;
751 Seierstad et al., 2014) used as reference for air T and rapid climatic variations. GS, Greenland
752 Stadials (1 to 26). NPs occurrences modified from Brocheray et al., 2014. Age of events after
753 Gottschalk et al., 2015. C17 to C20 are cold intervals for MIS4-MIS 5a (Sanchez-Goñi et al.,
754 2013).

Figure 3. Age model for core PP10-17 based on 38 dates (Tab. 1). A. Correlation age-depth. Horizontal scale with studied samples (cm; for clarity, only one of two samples have been displayed), grouped into stratigraphic units. Position of main events is indicated. Vertical shaded columns are Heinrich stadials after (Nps) maxima as indicated in Fig. 2. Dates are AMS ^{14}C datations (wide rectangles), tie-points with core MD95-2002 (black rectangles), with NGRIP (triangles) and Martinson et al. (1987; diamonds) (after Brocheray et al., 2014). Tie-points in vertical scale are taken from Otvos (2014), Gottschalk et al. (2015) and Naughton et al. (2016).B. Linear Least Squares Regression of age-depth values of core PP10-17 shows a good correlation (r = 0.96), though the best fit is performed with nonlinear logistic analysis (Fig. 3C). Software used is PAST 3 (Hammer et al., 2001).

Figure 4. Foraminifers in core PP10-17. A. Oceanity Index (OI, nº planktonic forams/total forams %) an estimation of the relative eustatic level. B. Benthic foraminifer species (with error bars) present in these samples, indicative of richness in benthic ecosystems. C. Benthic foraminifer coastal species (see Table 2), with marked shifts at the end of MIS6 and Bølling-Allerød, produced by inputs from shallower waters. In bottom of figure, core samples with dates, Greenland interstadials (GI) and shifts of Nps (representing cold intervals, see Fig. 2) are indicated for comparison.

Figure 5. Occurrence in core PP10-17 of major benthic foraminifer species *Cibicides wuellestorfi, Bulimina gibba + aculeata, Melonis barleeanus* and *Melonis pompilioides*. Bottom of figure as indicated in Fig. 4.

Figure 6. Occurrence in core PP10-17 of major benthic foraminifer species *Cassidulina laevigata, Globobulimina affinis, Uvigerina peregrina* and *Pyrgo murrhina* + spp. Bottom of figure as indicated in Fig. 4.

Figure 7. Ostracods in core PP10-17. A. Number of individuals. B. Number of species. C. Shannon H index of species diversity: increasing trends indicate stabilization of benthic ecosystems. D. Equitability J index: values close to one indicate stable environment. Bottom of figure as indicated in Fig. 4. Databases for these indices in Appendix A.

Figure 8. Occurrence of major benthic ostracod species in core PP10-17. A. Record of the eight species of *Krithe* found in this core. B. *Krithe trinidadensis*. C. *Krithe aequabilis*. D. *Argilloecia acuminata*. Bottom of figure as indicated in Fig. 4.

Figure 9. Magnetic susceptibility SI in core PP10-17. Major shifts are located at the end of Heinrich events H1 to H5. Bottom of figure as indicated in Fig. 4.

Figure 10. Element content (3-point average) of Ca, Sr, Ti and Fe in core PP10-17. Bottom of figure as indicated in Fig. 4.

Figure 11. Benthic foraminifer (BF) oxygen-content assemblages and diversity in core PP10-17 (see also Table 2). A. Oxic assemblage. B. Suboxic assemblage. C. Disoxic assemblage. D. BF Equitability J index. E. BF Shannon H species diversity index. Bottom of figure as indicated in Fig. 4. Databases for these indices in Appendix A.

Figure 12. Synthetic data of the proxies used in this work, including characteristic assemblages and diversities of planktonics foraminifers, benthic forams and ostracods, susceptibility and element content. Blue rectangles are Nps shifts in core PP10-17, indicative of cold SST in Central West Atlantic.

Oxygen content: O, oxic; S, suboxic; D, dysoxic. Benthic signal: +, increase; -, decrease. Productivity: OM, high organic matter; UP, upwelling; MES, mesotrophic. Benthic microhabitat: DI, deep infaunal; II, intermediate infaunal; SI, shallow infaunal.

Table Captions

Table 1. Dates used for the correlation age-depth in core PP10-17.

Table 2. Benthic foraminifer assemblages used in this work. A. Benthic foraminifer coastal species present in core PP10-17, used in Fig. 4C. The list includes species living in coastal and estuarine settlements of Bay of Biscay (Pascual et al., 2008; Martinez-Garcia et al., 2013). B. Benthic foraminifer assemblages indicative of oxygen content (after Kahio, 1994, 1999).

Table 3. Ecological preferences of the most characteristic benthic foraminifer species in core PP10-17. Dissolved oxygen levels after Kahio (1994, 1999).

Appendix A. Diversity databases of benthic foraminifer and ostracod assemblages. Data processed with PAST 3 software (Hammer et al., 2001).

Appendix B. Taxonomic list of the ostracod species mentioned in this work

Ostracods

Argilloecia acuminata Mueller, 1894

Krithe aequabilis Ciampo, 1986

Krithe dolichodeira Bold, 1946

Krithe minima Coles, Whatley and Moguilevski, 1994

Krithe gr. *minima* Coles, Whatley and Moguilevski, 1994

Krithe morkhoveni Bold, 1960

Krithe pernoides (Bornemann, 1855)

Krithe trinidadensis Bold, 1958

Krithe sp. 1

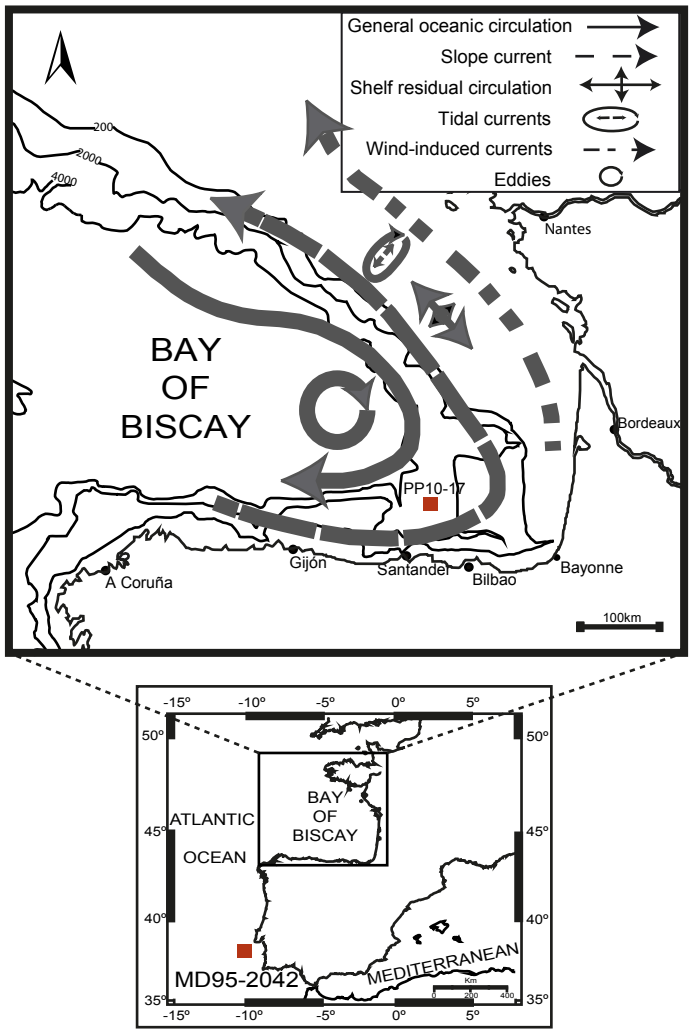
General oceanic circulation
Slope current
Shelf residual circulation
Tidal currents
Wind-induced currents
Eddies
200
2000
4000
BAY
OF
BISCAY
Nantes
Bordeaux
PP10-17
Gijón
Santander
Bilbao
Bayonne
A Coruña
100km
-15°
-10°
-5°
0°
5°
50°
45°
40°
35°
ATLANTIC
OCEAN
BAY
OF
BISCAY
MD95-2042
MEDITERRANEAN
Km
200
400

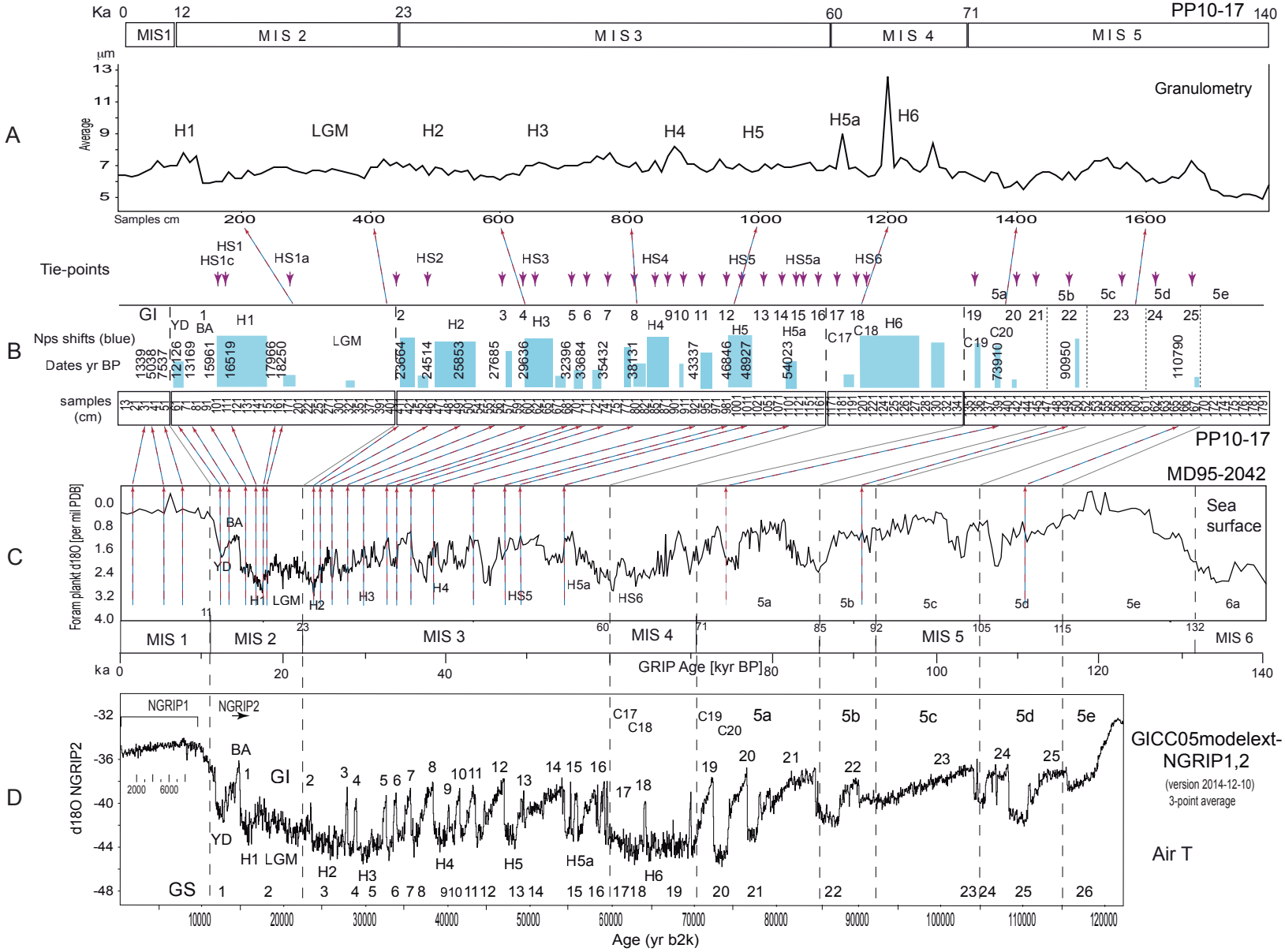
Ka 0 12 23 60 71 PP10-17 140
MIS1 MIS 2 MIS 3 MIS 4 MIS 5
A
µm
Granulometry
Average
H1 LGM H2 H3 H4 H5 H5a H6
Samples cm 200 400 600 800 1000 1200 1400 1600
Tie-points
HS1 HS1c HS1a HS2 HS3 HS4 HS5 HS5a HS6
GI
B
Nps shifts (blue)
Dates yr BP
samples (cm)
PP10-17
MD95-2042
C
Foram plankt d18O [per mil PDB]
Sea surface
MIS 1 MIS 2 MIS 3 MIS 4 MIS 5 MIS 6
ka 0 20 40 GRIP Age [kyr BP] 80 100 120 140
D
d18O NGRIP2
NGRIP1 NGRIP2
GI GS
Age (yr b2k)
GICC05modelext-NGRIP1,2
(version 2014-12-10)
3-point average
Air T

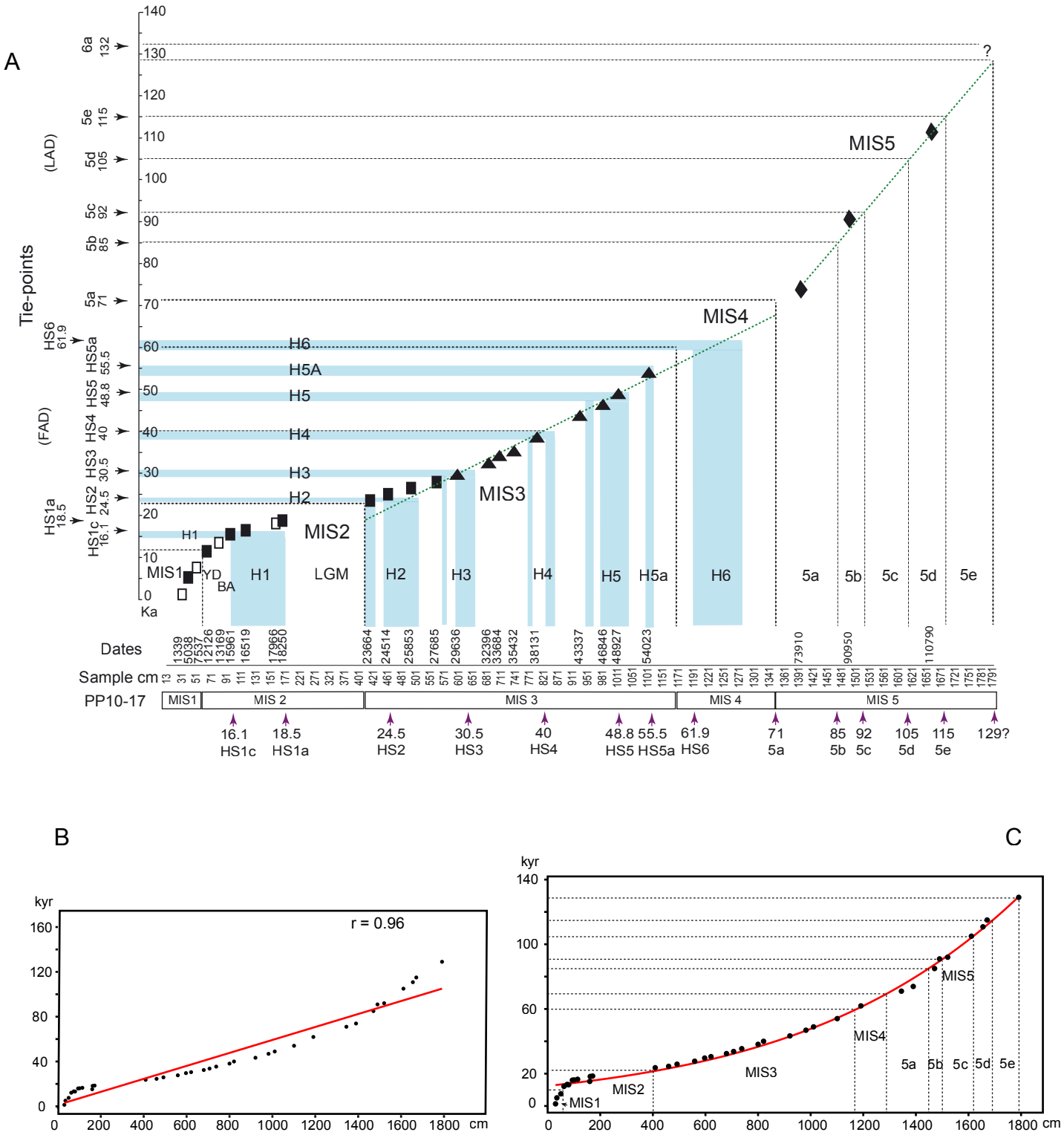
A
Tie-points
(LAD)
(FAD)
6a 132
5e 115
5d 105
5c 92
5b 85
5a 71
HS6 61.9
HS5a 55.5
HS5 48.8
HS4 40
HS3 30.5
HS2 24.5
HS1a 18.5
HS1c 16.1
Ka
MIS5
MIS4
MIS3
MIS2
MIS1
H6
H5A
H5
H4
H3
H2
H1
YD
BA
LGM
5a
5b
5c
5d
5e
Dates
Sample cm
PP10-17
MIS 2
MIS 3
MIS 4
MIS 5
16.1 HS1c
18.5 HS1a
24.5 HS2
30.5 HS3
40 HS4
48.8 HS5
55.5 HS5a
61.9 HS6
71 5a
85 5b
92 5c
105 5d
115 5e
129?
B
kyr
r = 0.96
cm
C
kyr
MIS1
MIS2
MIS3
MIS4
MIS5
5a
5b
5c
5d
5e
cm

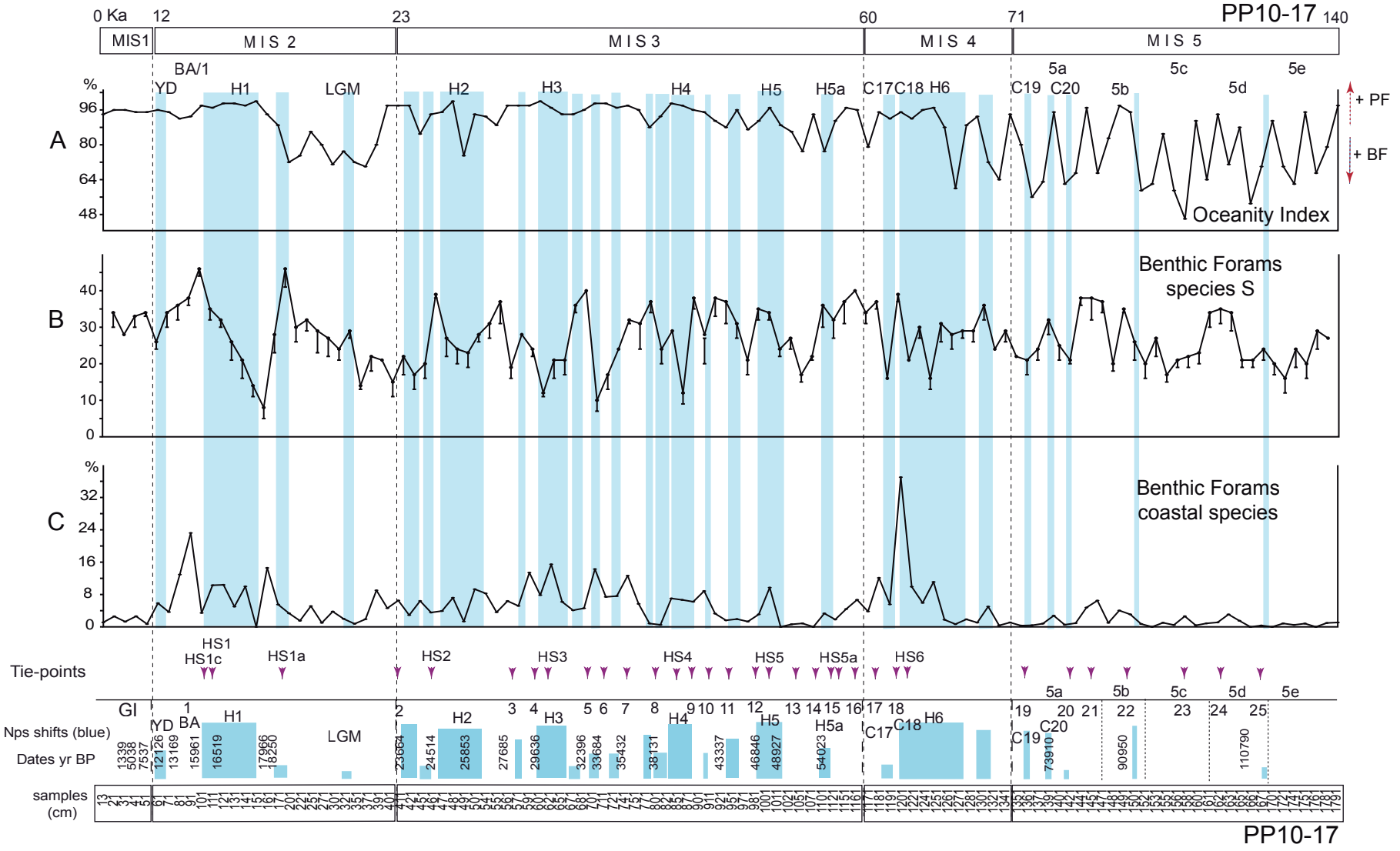
PP10-17
0 Ka
12
23
60
71
140
MIS1
MIS 2
MIS 3
MIS 4
MIS 5
BA/1
YD
H1
LGM
H2
H3
H4
H5
H5a
C17
C18
H6
C19
C20
5a
5b
5c
5d
5e
+ PF
+ BF
A
%
96
80
64
48
Oceanity Index
B
40
30
20
10
0
Benthic Forams
species S
C
%
32
24
16
8
0
Benthic Forams
coastal species
Tie-points
HS1
HS1c
HS1a
HS2
HS3
HS4
HS5
HS5a
HS6
GI
Nps shifts (blue)
Dates yr BP
1339
5038
7537
12126
13169
15961
16519
17966
18250
23664
24514
25853
27685
29636
32396
33684
35432
38131
43337
46846
48927
54023
73910
90950
110790
samples
(cm)
PP10-17

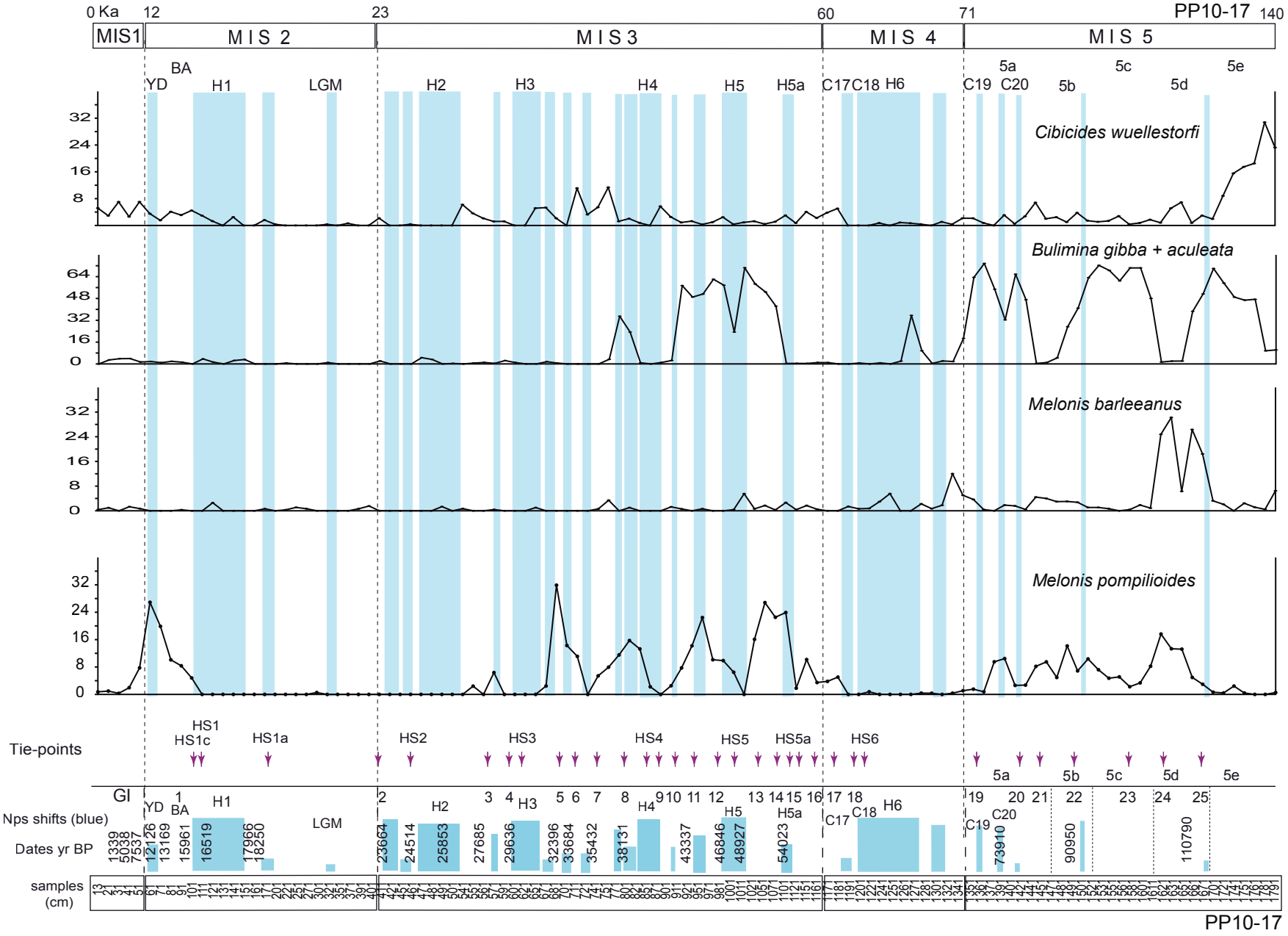
PP10-17
0 Ka
12
23
60
71
140
MIS1
M I S 2
M I S 3
M I S 4
M I S 5
BA
YD
H1
LGM
H2
H3
H4
H5
H5a
C17
C18
H6
C19
C20
5a
5b
5c
5d
5e
Cibicides wuellestorfi
Bulimina gibba + aculeata
Melonis barleeanus
Melonis pompilioides
Tie-points
HS1
HS1c
HS1a
HS2
HS3
HS4
HS5
HS5a
HS6
GI
Nps shifts (blue)
Dates yr BP
1339
5038
7537
12126
13169
15961
16519
17966
18250
23664
24514
25853
27685
29636
32396
33684
35432
38131
43337
46846
48927
54023
73910
90950
110790
samples
(cm)
PP10-17

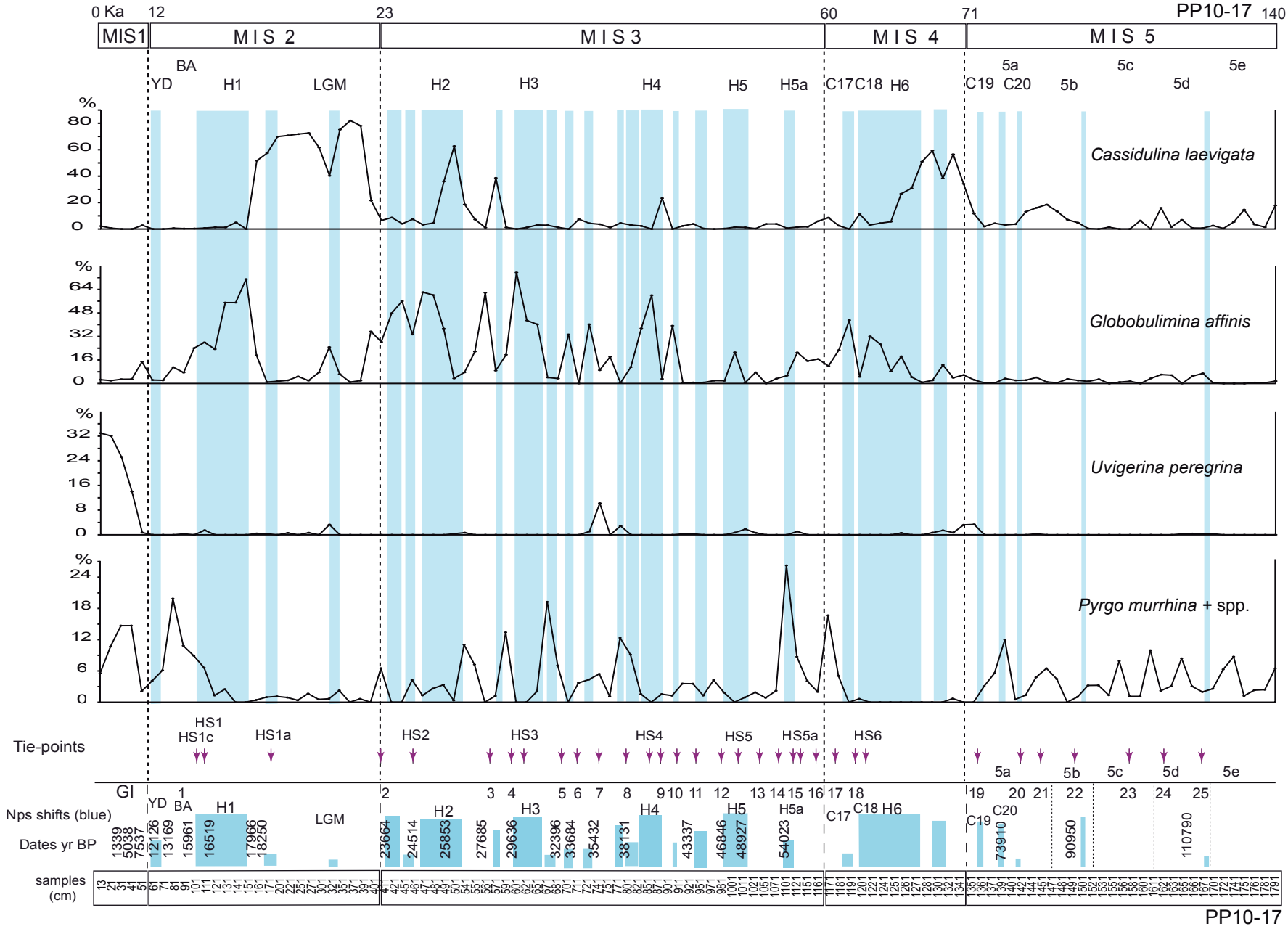
0 Ka
12
23
60
71
140
PP10-17
MIS1
MIS 2
MIS 3
MIS 4
MIS 5
BA
YD
H1
LGM
H2
H3
H4
H5
H5a
C17
C18
H6
C19
C20
5a
5b
5c
5d
5e
Cassidulina laevigata
Globobulimina affinis
Uvigerina peregrina
Pyrgo murrhina + spp.
%
Tie-points
HS1
HS1c
HS1a
HS2
HS3
HS4
HS5
HS5a
HS6
GI
Nps shifts (blue)
Dates yr BP
samples
(cm)
PP10-17

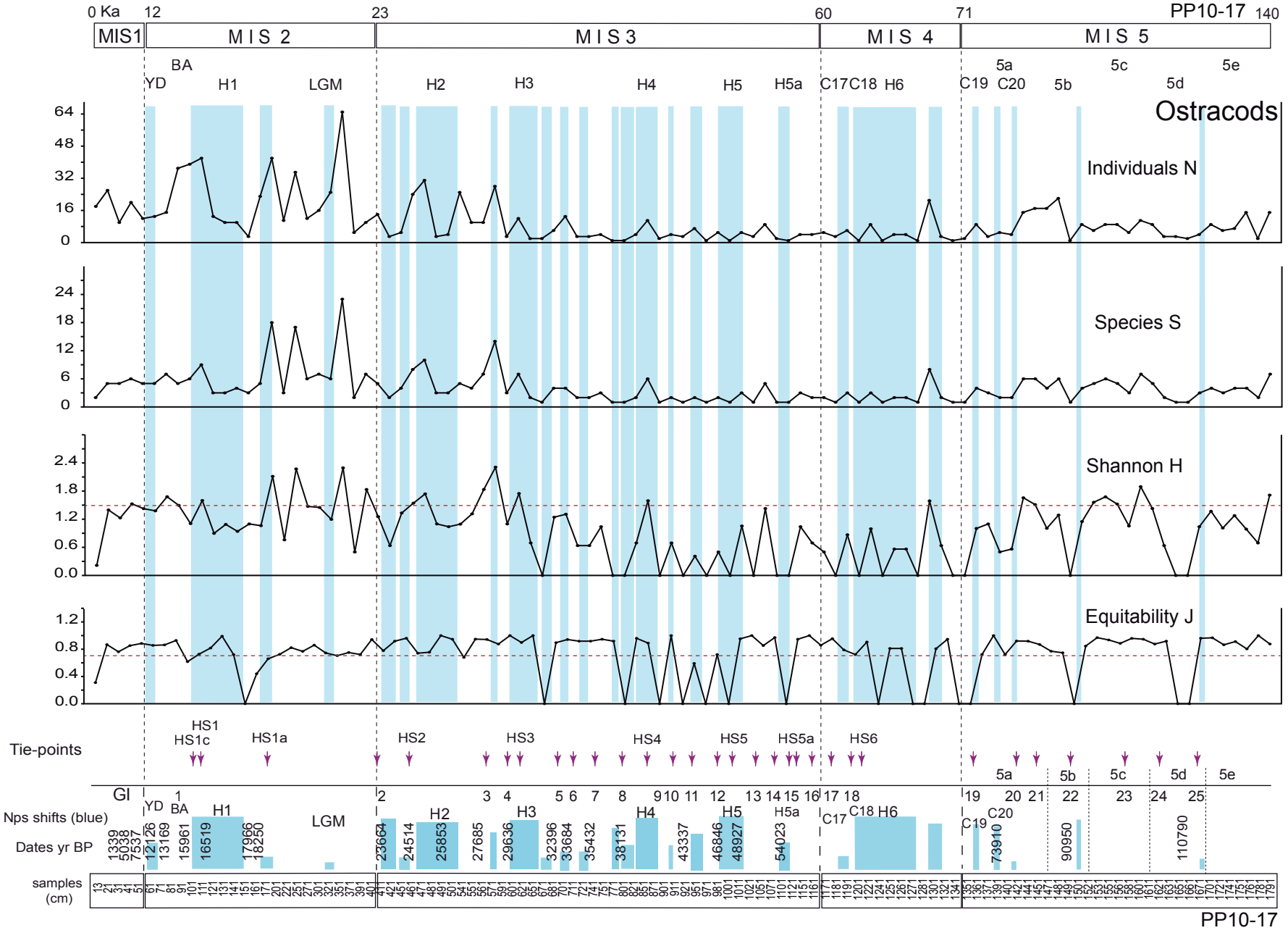
PP10-17
0 Ka
12
23
60
71
140
MIS1
M I S 2
M I S 3
M I S 4
M I S 5
BA
YD
H1
LGM
H2
H3
H4
H5
H5a
C17
C18
H6
C19
C20
5a
5b
5c
5d
5e
Ostracods
Individuals N
Species S
Shannon H
Equitability J
Tie-points
HS1
HS1c
HS1a
HS2
HS3
HS4
HS5
HS5a
HS6
GI
Nps shifts (blue)
Dates yr BP
samples (cm)
1339
5038
7537
12126
13169
15961
16519
17966
18250
23664
24514
25853
27685
29636
32396
33684
35432
38131
43337
46846
48927
54023
73910
90950
110790
PP10-17

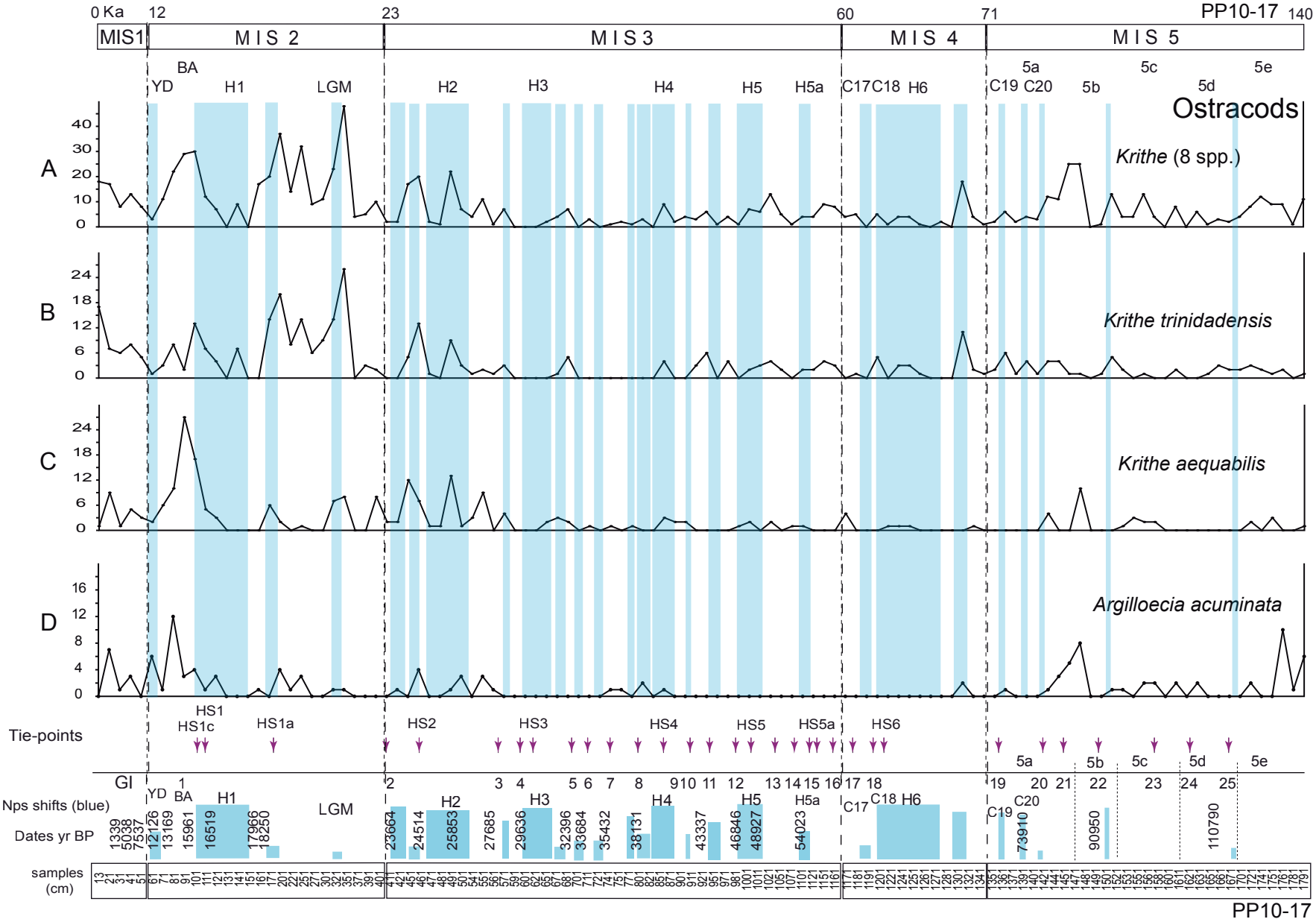
0 Ka
12
23
60
71
PP10-17
140
MIS1
M I S 2
M I S 3
M I S 4
M I S 5
BA
YD
H1
LGM
H2
H3
H4
H5
H5a
C17
C18
H6
C19
C20
5a
5b
5c
5d
5e
Ostracods
A
Krithe (8 spp.)
B
Krithe trinidadensis
C
Krithe aequabilis
D
Argilloecia acuminata
Tie-points
HS1
HS1c
HS1a
HS2
HS3
HS4
HS5
HS5a
HS6
GI
Nps shifts (blue)
Dates yr BP
samples
(cm)
1339
5038
7537
12126
13169
15961
16519
17966
18250
23664
24514
25853
27685
29636
32396
33684
35432
38131
43337
46846
48927
54023
73910
90950
110790
PP10-17

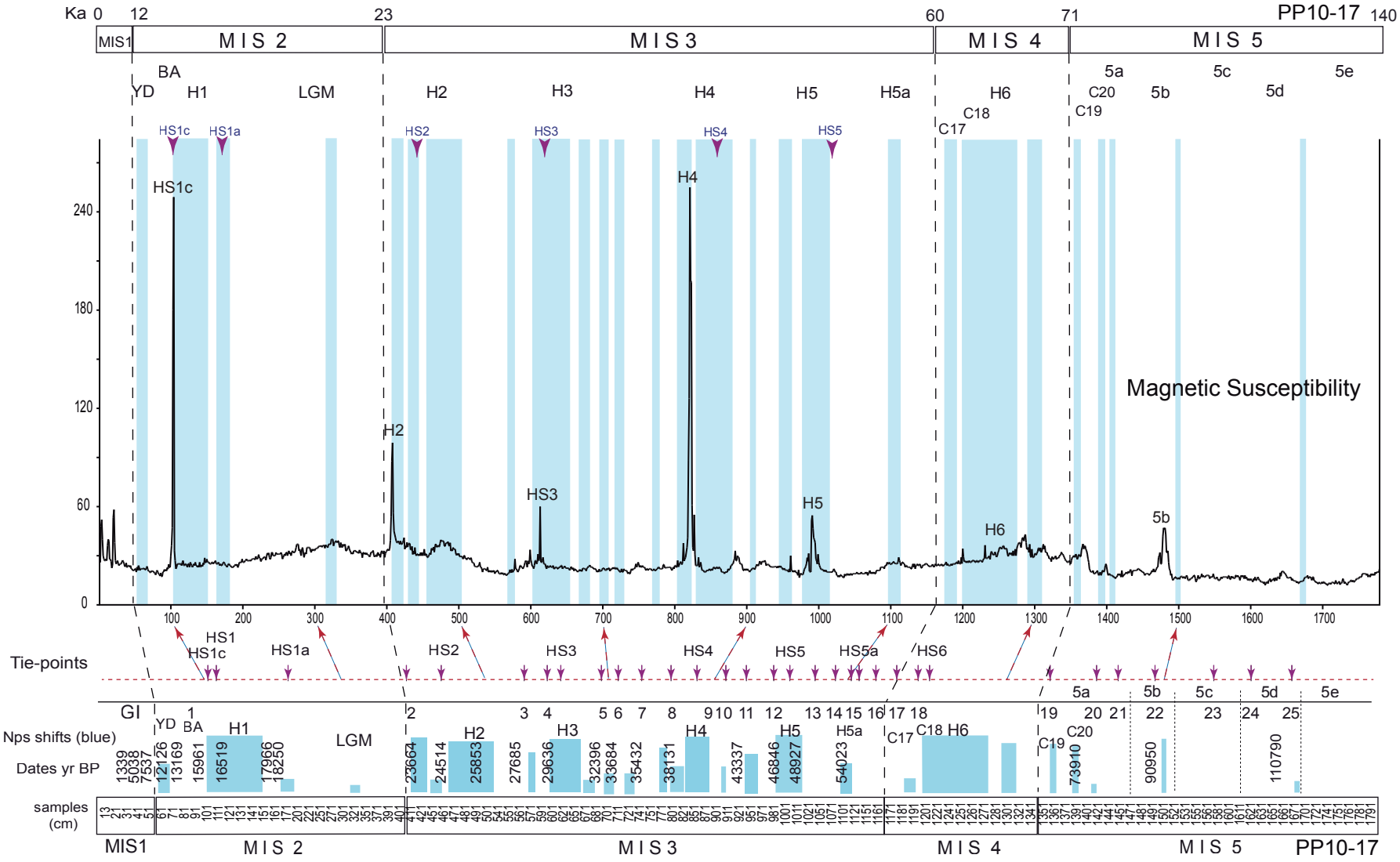
Ka 0
12
23
60
71
140
PP10-17
MIS1
MIS 2
MIS 3
MIS 4
MIS 5
BA
YD
H1
LGM
H2
H3
H4
H5
H5a
H6
C17
C18
C19
C20
5a
5b
5c
5d
5e
HS1c
HS1a
HS2
HS3
HS4
HS5
Magnetic Susceptibility
240
180
120
60
0
100
200
300
400
500
600
700
800
900
1000
1100
1200
1300
1400
1500
1600
1700
Tie-points
HS1
HS5a
HS6
GI
1
2
3
4
5
6
7
8
9
10
11
12
13
14
15
16
17
18
19
20
21
22
23
24
25
Nps shifts (blue)
Dates yr BP
1339
5038
7537
12126
13169
15961
16519
17966
18250
23664
24514
25853
27685
29636
32396
33684
35432
38131
43337
46846
48927
54023
73910
90950
110790
samples
(cm)
MIS1
MIS 2
MIS 3
MIS 4
MIS 5
PP10-17

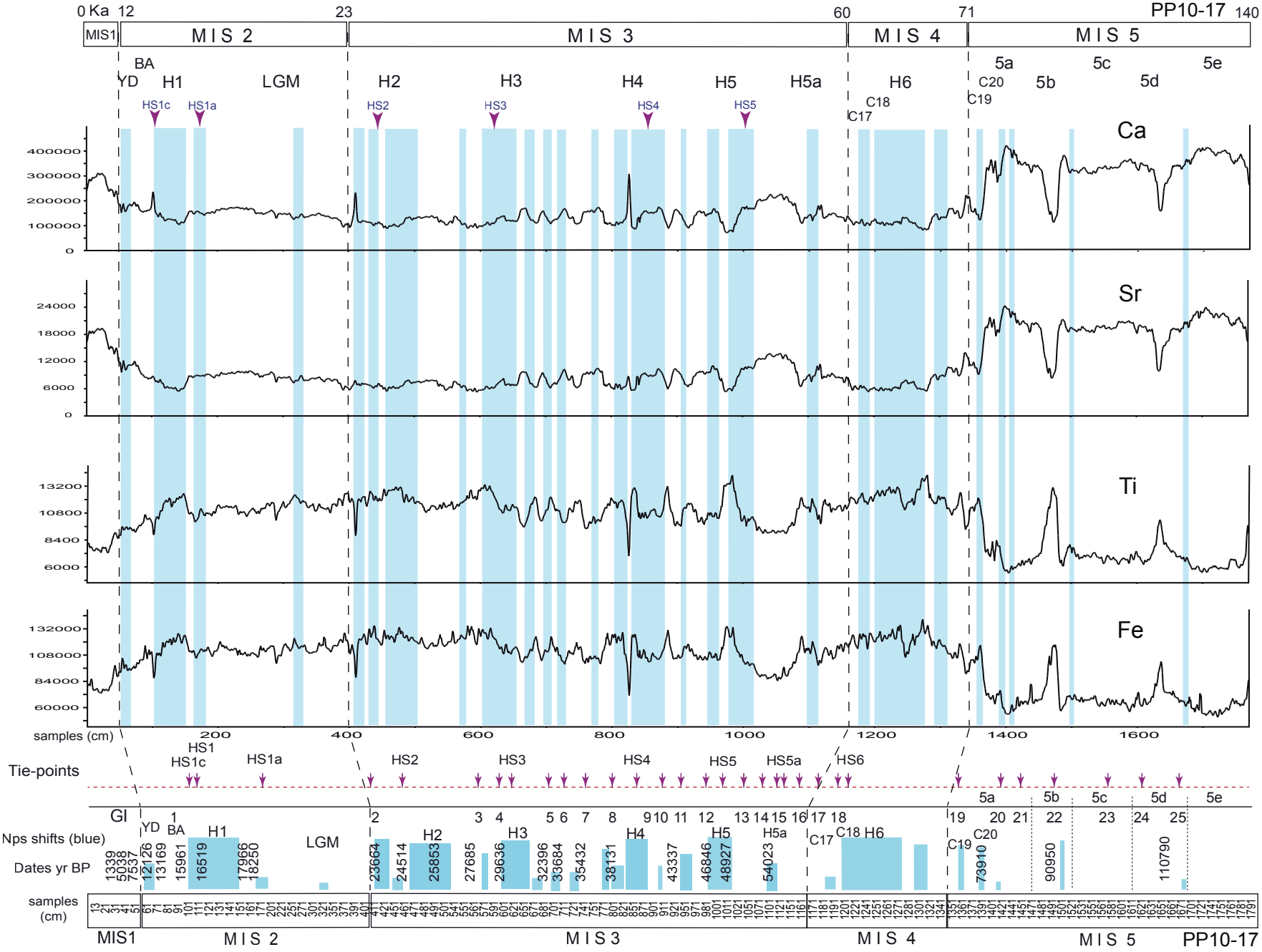
0 Ka
12
23
60
71
140
PP10-17
MIS1
MIS 2
MIS 3
MIS 4
MIS 5
BA
YD
H1
LGM
H2
H3
H4
H5
H5a
H6
C20
C19
C18
C17
5a
5b
5c
5d
5e
HS1c
HS1a
HS2
HS3
HS4
HS5
Ca
Sr
Ti
Fe
samples (cm)
Tie-points
HS1
HS6
GI
Nps shifts (blue)
Dates yr BP
samples (cm)
MIS1
MIS 2
MIS 3
MIS 4
MIS 5
PP10-17

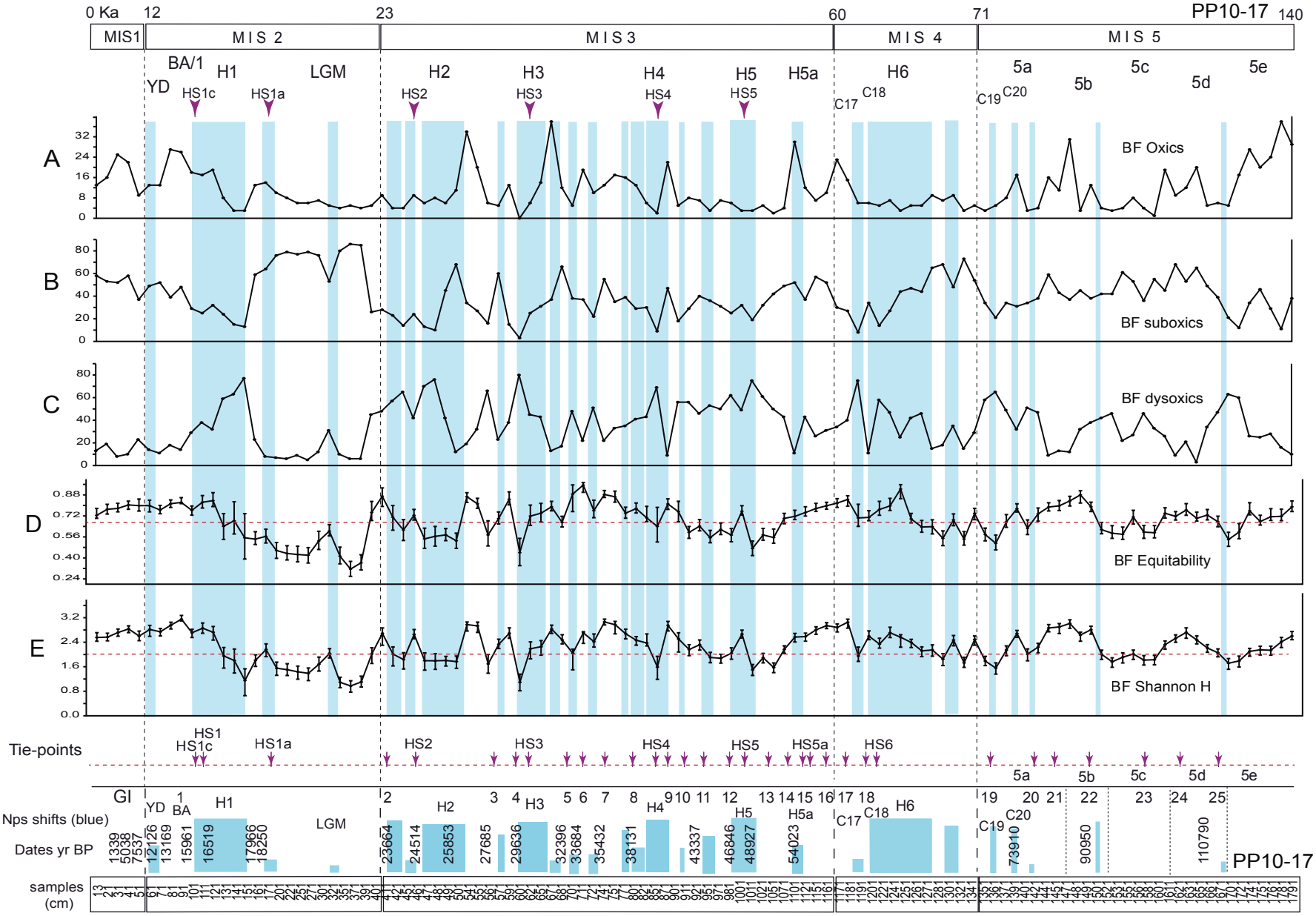
0 Ka
12
23
60
71
140
PP10-17
MIS1
MIS 2
MIS 3
MIS 4
MIS 5
BA/1
YD
H1
LGM
H2
H3
H4
H5
H5a
H6
5a
5b
5c
5d
5e
HS1c
HS1a
HS2
HS3
HS4
HS5
C17
C18
C19
C20
A
BF Oxics
B
BF suboxics
C
BF dysoxics
D
BF Equitability
E
BF Shannon H
Tie-points
HS1
HS6
GI
1
2
3
4
5
6
7
8
9
10
11
12
13
14
15
16
17
18
19
20
21
22
23
24
25
Nps shifts (blue)
Dates yr BP
1339
5038
7537
12126
13169
15961
16519
17966
18250
23664
24514
25853
27685
29636
32396
33684
35432
38131
43337
46846
48927
54023
73910
90950
110790
PP10-17
samples
(cm)

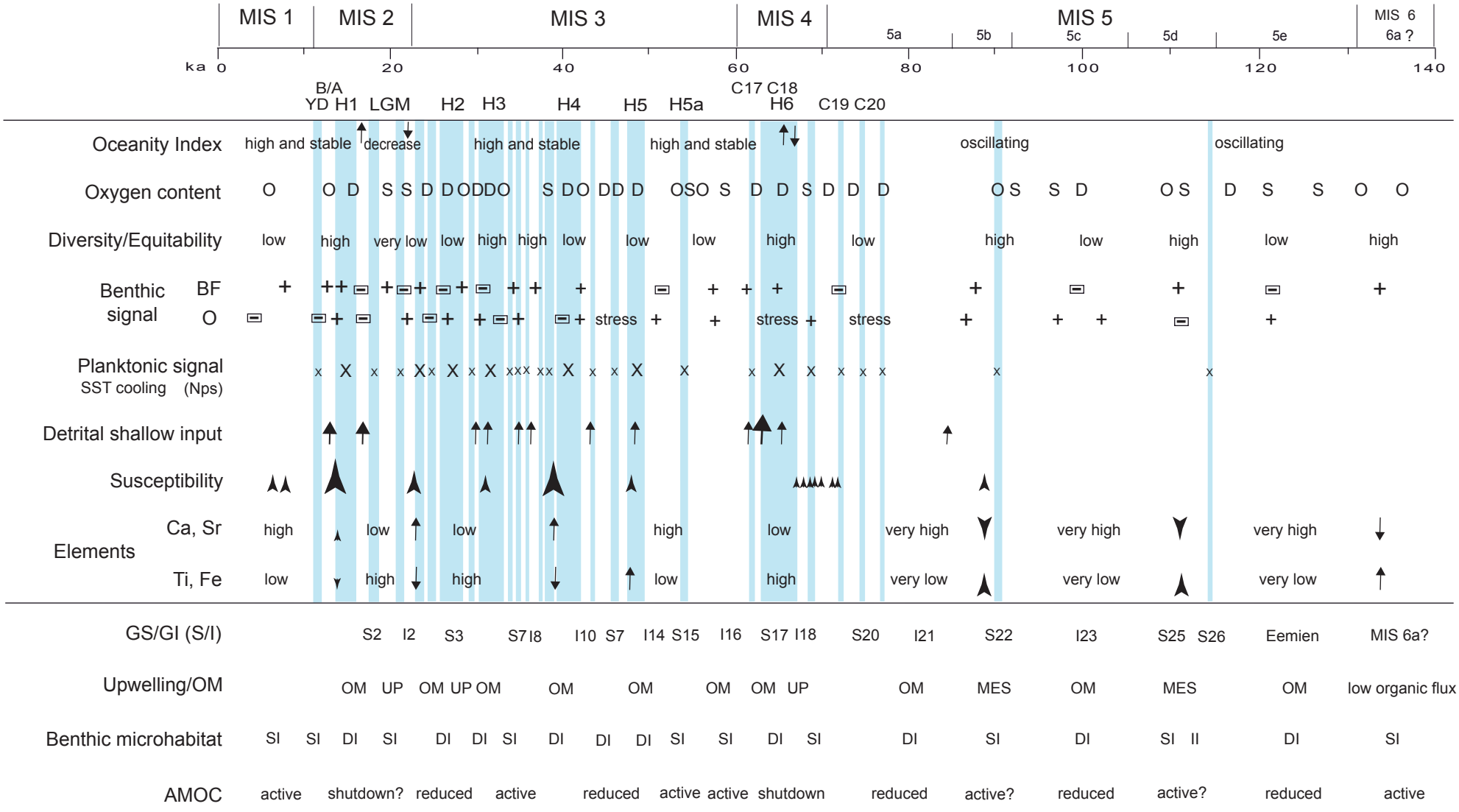
MIS 1
MIS 2
MIS 3
MIS 4
MIS 5
5a
5b
5c
5d
5e
MIS 6
6a ?
ka 0
20
40
60
80
100
120
140
B/A
YD H1 LGM H2 H3 H4 H5 H5a
C17 C18
H6
C19 C20
Oceanity Index
high and stable
decrease
high and stable
high and stable
oscillating
oscillating
Oxygen content
Diversity/Equitability
Benthic signal
BF
O
stress
Planktonic signal
SST cooling (Nps)
Detrital shallow input
Susceptibility
Elements
Ca, Sr
Ti, Fe
GS/GI (S/I)
S2 I2 S3 S7 I8 I10 S7 I14 S15 I16 S17 I18 S20 I21 S22 I23 S25 S26 Eemien MIS 6a?
Upwelling/OM
Benthic microhabitat
AMOC
active
shutdown?
reduced
active
reduced
active
active
shutdown
reduced
active?
reduced
active?
reduced
active

Core depth (cm)	Date Calendar age BP (years)	Stratigraphic correlation	Datation (D)/ Tie-point (T)	Reference
30	1339	AMS ^{14}C	D	Brocheray et al., 2014
35	5038	MD95-2002	T	Brocheray et al., 2014
50	7537	AMS ^{14}C	D	Brocheray et al., 2014
62	12126	MD95-2002	T	Brocheray et al., 2014
74	13338	MD95-2002	T	Brocheray et al., 2014
80	13169	AMS ^{14}C	D	Brocheray et al., 2014
94	15961	MD95-2002	T	Brocheray et al., 2014
101	16100	HS1c	T	Naughton et al., 2016
114	16519	MD95-2002	T	Brocheray et al., 2014
160	17966	AMS ^{14}C	D	Brocheray et al., 2014
162	18250	MD95-2002	T	Brocheray et al., 2014
171	18500	HS1a	T	Naughton et al., 2016
409	23664	MD95-2002	T	Brocheray et al., 2014
460	24514	MD95-2002	T	Brocheray et al., 2014
492	25853	MD95-2002	T	Brocheray et al., 2014
559	27685	MD95-2002	T	Brocheray et al., 2014
597	29636	NGRIP	T	Brocheray et al., 2014
621	30500	HS3	T	Gottschalk et al., 2015
680	32396	NGRIP	T	Brocheray et al., 2014
707	33684	NGRIP	T	Brocheray et al., 2014
738	35432	NGRIP	T	Brocheray et al., 2014
800	38131	NGRIP	T	Brocheray et al., 2014
821	39800	HS4	T	Gottschalk et al., 2015
921	43337	NGRIP	T	Brocheray et al., 2014
982	46846	NGRIP	T	Brocheray et al., 2014
1001	48600	HS5	T	Gottschalk et al., 2015
1011	48927	NGRIP	T	Brocheray et al., 2014
1101	54023	NGRIP	T	Brocheray et al., 2014
1191	61900	HS6	T	Gottschalk et al., 2015
1345	71000	MIS 5a	T	Otvos, 2014
1390	73910	Martinson et al., 1987	T	Brocheray et al., 2014
1471	85000	MIS 5b	T	Otvos, 2014
1490	90950	Martinson et al., 1987	T	Brocheray et al., 2014
1521	92000	MIS 5c	T	Otvos, 2014
1611	105000	MIS 5d	T	Otvos, 2014
1655	110790	Martinson et al., 1987	T	Brocheray et al., 2014
1671	115000	MIS 5e	T	Otvos, 2014
1791	129000	MIS 5e	T	Otvos, 2014

Table 1. Dates used for the correlation age-depth in core PP10-17.

A. Benthic foraminifer coastal species	Benthic Foraminifer oxygen content indicators		
	Oxia indicators (>1.5 ml/l O2)	Suboxia indicators (0.3-1.5 ml/l O2)	Dysoxia indicators (0.1-0.3 ml/l O2)
Ammonia beccarii (Linné, 1758)	*Bulimina truncana* Gumbel, 1868	*Bolivinita quadrilatera* (Schwager, 1866)	*Bolivina alata* (Seguenza, 1862)
Ammonia sp.	*Cibicides floridanus* (Cushman, 1918)	*Bulimina aculeata* d'Orbigny, 1826	*Bolivina difformis* (Williamson, 1858)
Asterigerinata mamilla (Williamson, 1858)	*Cibicides refulgens* de Montfort, 1808	*Bulimina striata* d'Orbigny, in Guérin-Méneville, 1843	*Bolivina dilatata* Reuss, 1850
Asterigerinata sp.	*Cibicides wuellerstorfi* (Schwager, 1866)	*Cassidulina laevigata* d'Orbigny, 1826	*Bolivina earlandi* Parr, 1950
Cribroelphidium excavatum (Terquem, 1875)	*Cibicides* sp.	*Cribroelphidium excavatum* (Terquem, 1875)	*Bolivina pseudoplicata* Heron-Allen & Earland, 1930
Elphidium crispum (Linné, 1758)	*Cibicidoides pseudoungeriana* (Cushman, 1922)	*Fissurina formosa* (Schwager, 1866)	*Bolivina pygmaea* (Brady, 1881)
Elphidium gerthi Van Voorthuysen, 1957	*Cibicidoides robertsoniana* (Brady, 1881)	*Fissurina lucida* (Williamson, 1848)	*Bolivina spathulata* (Williamson, 1858)
Haynesina depressula (Walker & Jacob, 1798)	*Cibicidoides* sp.	*Fissurina marginata* (Montagu, 1803)	*Bolivina subaenariensis* Cushman, 1922
Lobatula lobatula (Walker & Jacob, 1798)	*Globocassidulina subglobosa* (Brady, 1881)	*Fissurina orbignyana* Seguenza, 1862	*Bulimina gibba* Fornasini, 1902
Miliolinella subrotunda (Montagu, 1803)	*Osangularia culter* (Parker & Jones, 1865)	*Fissurina pseudoorbignyana* (Buchner, 1940)	*Bulimina inflata* Seguenza, 1862
Nonion commune (d'Orbigny, 1846)	*Lobatula lobatula* (Walker & Jacob, 1798)	*Fissurina seminiformis* (Schwager, 1866)	*Bulimina marginata* d'Orbigny, 1826
Quinqueloculina lata Terquem, 1876	*Pyrgo murrhina* (Schwager, 1866)	*Gyroidina* sp.	*Chilostomella oolina* Schwager, 1878
Quinqueloculina seminula (Linnaeus, 1758)	*Quinqueloculina lamarckiana* d'Orbigny, 1839	*Hansenisca soldanii* (d'Orbigny, 1826)	*Chilostomella ovoidea* Reuss, 1850
Rosalina globularis d'Orbigny, 1826	*Quinqueloculina lata* Terquem, 1876	*Hoeglundina elegans* (d'Orbigny, 1878)	*Dentalina mutabilis* (Costa, 1855)
Rosalina sp.	*Quinqueloculina seminula* (Linnaeus, 1758)	*Laevidentalina inornata* (d'Orbigny, 1846)	*Dentalina* sp.
Triloculina oblonga (Montagu, 1803)	*Triloculina oblonga* (Montagu, 1803)	*Laevidentalina communis* (d'Orbigny, 1826)	*Eubuliminella exilis* (Brady, 1884)
	Triloculina tricarinata d'Orbigny, 1826	*Lagena apiculata* (Reuss, 1851)	*Fursenkoina complanata* (Egger, 1893)
		Lagena elongata Dunikowski, 1879	*Fursenkoina* sp.
		Lagena gibbera Buchner, 1940	*Globobulimina affinis* (d'Orbigny, 1839)
		Lagena hispida Reuss, 1858	*Globobulimina auriculata* (Bailey, 1894)
		Lagena semistriata Williamson, 1848	*Globobulimina* sp. cf. *pacifica* Cushman, 1927
		Lagena staphyllearia (Schwager, 1866)	
		Lagena striata (d'Orbigny, 1839)	
		Lagena substriata Williamson, 1848	
		Lagena sulcata (Walker & Jacob, 1798)	
		Lenticulina articulata (Terquem, 1862)	
		Lenticulina gibba (d'Orbigny, 1826)	
		Lenticulina inornata (d'Orbigny, 1846)	
		Lenticulina iota (Cushman, 1923)	
		Lenticulina orbicularis (d'Orbigny, 1826)	
		Lenticulina sp.	
		Melonis barleeanus (Williamson, 1858)	
		Melonis pompilioides (Fichtel & Moll, 1798)	
		Neolenticulina peregrina (Schwager, 1866)	
		Nonion commune (d'Orbigny, 1846)	
		Nonion sp.	
		Nonionella atlantica Cushman, 1936	
		Oridorsalis umbonatus (Reuss, 1851)	
		Procerolagena gracilis (Williamson, 1848)	
		*Pullenia bulloide*s (d'Orbigny, 1846)	
		Pullenia quinqueloba (Reuss, 1851)	
		Pullenia salisburyi Stewart & Stewart, 1930	
		Trifarina angulosa (Williamson, 1858)	
		Trifarina bradyi Cushman, 1923	
		Uvigerina auberiana d'Orbigny, 1839	
		Uvigerina cushmani Todd, 194	
		Uvigerina peregrina Cushman, 1923	
		Valvulineria bradyana (Fornasini, 1900)	

Table 2. Benthic foraminifer assemblages used in this work. A. Benthic foraminifer coastal species present in core PP10-17, used in Fig. 4C. The list includes species living in coastal and estuarine settlements of Bay of Biscay (Pascual et al., 2008; Martinez-Garcia et al., 2013). B. Benthic foraminifer assemblages indicative of oxygen content (after Kahio, 1994, 1999).

Species	Dissolved-oxygen	Microhabitat	Ecological preference
Cibicides wuellerstorfi (Schwager, 1866)	Oxic (> 2ml/l)	Shallow infaunal (Fontanier et al, 2003)	Cold (-2 to 4ºC) and deep water (1360-4280 m) (Murray, 1991), high oxygen content (>2ml/l) (Kahio, 1994, Schmield et al., 1997). OM flux relatively low (Gooday, 2003) locally adapted to pulses of organic carbon (De and Gupta 2010; Diz and Barker, 2016). Increasing of its occurrence in the paleo-assemblages is indicative of increasing of deep bottom waters (Bornmalm et al., 1999). This species is associated with NADW (North Atlantic Deep Water) and ACW (Antarctic Circumpolar Water) (Douglas and Woodruff, 1981; Murray, 1991).
Bulimina gibba Fornasini, 1902	Disoxic (0.1-0.3 ml/l)	Deep infaunal (Mendes et al., 2004)	In this core, two main species of *Bulimina* (*B. gibba, B. aculeata*) are cool-temperate (5-17ºC) (Murray, 1991) and high productivity waters (Ray and Singh, 2012). In particular, *B. gibba* is typical of strongly eutrophic and anoxic environments (Fontanier et al., 2002).
Bulimina aculeata d'Orbigny, 1826	Suboxic (0.3-1.5ml/l)	Deep infaunal (Fontanier et. al, 2002; Rai and Singh, 2012)	*Bulimina aculeata* is associated to elevated fluxes of organic carbon in bathyal waters (Mackensen et al., 1990; Wells et al., 1994).
Melonis barleeanus (Williamson, 1858)	Suboxic	Shallow infaunal /Intermediate infaunal (Fontanier et al., 2003; Grunert et al, 2015)	*Melonis barleeanus* is a cold water species (-0.4 to 9ºC), with depth range 280 to 2710 m (Murray, 1991). It tolerates high concentrations of OM (Fontanier et al., 2002). It is present in virtual absence of oxygen and low nitrates (Jorissen et al., 1998). Indicative of deep mesotrophic conditions (Jorissen, 2003; Grunert et al., 2015).
Melonis pompilioides (Fichtel and Moll, 1798)	Suboxic	Shallow infaunal (Mojtahid et al., 2010). Intermediate infaunal (Grunert et al., 2015)	*Melonis pompilioides* is a cold water species (4.9ºC) (Frerichs, 1970), oportunistic adapted to high concentration of food and tolerates high organic detritus fluxes (Baas et al., 1998), typically occurring during cold intervals in cores (Corliss, 1983). Shifts of this species are related with the entrance of OM (Grunert et al., 2015).
Cassidulina laevigata d'Orbigny, 1826	Suboxic	Shallow infaunal (Fontanier et al, 2002)	*C. laevigata* has been related with upwelling (Levy et al., 1995). It is an oportunistic species adapted to high food content (Baas et al., 1998), with high organic carbon flux (>3 gC/m/yr) (Jorissen et al., 2007). It is also present in areas of seasonal flux of OM (Rasmusen et al., 2002). In Portugal it is present in glacial periods, with shifts of paleoproductivity (Baas et al., 1998). This species (as *C. carinata)* was abundant during MIS 2 and MIS 4 in the Mediterranean (Singh et al., 2015).
Globobulimina affinis (d'Orbigny, 1839)	Disoxic	Deep infaunal (Fontanier et al, 2003; Geslin et al., 2004)	*Globobulimina* is a cold water genus. *Gl. affinis* is a bathyal species living in sediments with high OM content (Fontanier et al., 2005). It is cosmopolitan in areas of high productivity, high carbon content and disoxic waters (Hayek and Wilson, 2013; Patarroyo and Martinez, 2016), but prefers anoxic conditions (Geslin et al., 2004; Fontanier et al., 2002), by active migration inside the sediment to find this anoxic preferred habitat (Geslin et al., 2004). This low-oxygen adaptation makes this species a good proxy for strongly disoxic environments (Schonfeld, 2001; Jorissen et al., 2007; Grunert et al., 2015). It is present in HE4 in Portugal (Bas et al., 1998), and HE1, HE4 with IRD shift in the Bay of Biscay (Loncaric et al., 1998).
Uvigerina peregrina Cushman, 1923	Suboxic	Shallow infaunal/ Intermediate infaunal (Fontanier et al., 2002, 2003)	*Uvigerina peregrina* is a temperate (6-15ºC) species (Murray, 1991), indicative of high productivity waters (Lutze, 1986; Ray and Singh, 2012; Patarroyo and Martinez, 2016), and positively correlated with OM in the sediment (Fontanier et al., 2002). This is a dominant species when organic carbon flux exceeded 2-3 g/m2a (Altenbach, 1988). Tolerates virtual absence of oxygen (Lohmann, 1978), becoming dominant in upwelling areas (Debenay and Konate, 1987). Thus, the abundance of *Uvigerina peregrina* suggests seasonal phytodetritus fluxes exported from surface with strong seasonal productivity (García et al., 2013). *U. peregrina* is one of the species that better tolerates the low quality of OM, characterising mesotrophic and oligotrophic environments (Mojtahid et al., 2010). It is influenced by the upper NADW or CDW (Circumpolar Deep Water) (Schnitker, 1979).
Pyrgo murrhina (Schwager, 1866)	Oxic	Shallow infaunal (Kuhnt et al., 2007)	*Pyrgo murrhina* is a cold water (<3ºC) species (Murgese and De Deckker, 2005), living in bathyal Atlantic (Gudmundsson, 1998), in areas with low organic carbon flux and high oxygen content (>3.5 ml/l) (Altenbach et al., 1999; Murgese and De Deckker, 2005). It has been related with periods of increasing deep water formation with nutrient increase (Bornmalm et al., 1999). It is living in oligotrophic environments (García et al., 2013). Present in glacial stages of Portugal (Baas et al., 1998).This species is a good proxy of oxygen waters (Caulle et al., 2014), being almost absent when the waters become disoxic.

Table 3. Ecological preferences of the most characteristic benthic foraminifer species in core PP10-17. Dissolved oxygen levels after Kahio (1994, 1999).

BENTHIC FORAMS

cm core	13	21	31	41	51	61	71	81	91	101	111	121	131	141	151	161	171	201	221	251
Taxa_S	34	28	33	34	26	34	36	38	46	35	32	26	21	14	8	28	46	30	32	29
Individuals	270	309	313	306	142	171	324	317	323	291	136	77	80	40	31	240	308	269	332	273
Dominance_D	0.1453	0.1367	0.1084	0.08932	0.1149	0.1076	0.1047	0.07926	0.05992	0.1109	0.1058	0.1017	0.3175	0.3212	0.5172	0.3126	0.3376	0.4933	0.5063	0.521
Shannon_H	2,555	2,567	2,717	2,833	2,601	2,816	2,741	2,957	3.15	2.71	2,857	2,725	1,952	1,802	1,151	1.81	2,161	1,553	1,505	1,434
Equitability_J	0.7245	0.7702	0.7771	0.8035	0.7982	0.7985	0.765	0.8128	0.8229	0.7622	0.8243	0.8363	0.6411	0.683	0.5535	0.5432	0.5644	0.4565	0.4341	0.426

cm core	271	301	321	351	371	391	401	411	421	451	461	471	481	491	501	541	551	561	571	591
Taxa_S	27	24	29	14	22	21	15	22	17	20	39	27	24	23	28	31	37	19	28	24
Individuals	303	185	303	266	317	310	65	46	69	125	282	153	153	300	290	145	166	94	251	82
Dominance_D	0.5326	0.3951	0.2352	0.5746	0.6752	0.6142	0.1976	0.1115	0.256	0.3315	0.1444	0.3947	0.3743	0.2752	0.4026	0.07434	0.08804	0.3929	0.1851	0.09607
Shannon_H	1,386	1,683	2,035	1.09	0.9741	1,103	2,021	2,689	2,013	1,835	2,655	1,797	1,793	1,804	1,768	2,976	2,932	1,694	2,331	2,692
Equitability_J	0.4206	0.5295	0.6043	0.4132	0.3151	0.3623	0.7461	0.87	0.7104	0.6125	0.7247	0.5453	0.5643	0.5754	0.5306	0.8665	0.8119	0.5753	0.6996	0.847

cm core	601	621	651	671	681	701	711	721	741	751	771	801	821	851	871	901	911	921	951	971
Taxa_S	12	21	21	36	40	10	17	24	32	31	37	24	29	12	38	28	38	37	31	21
Individuals	102	84	97	244	326	21	27	101	166	88	243	197	128	45	193	79	336	310	312	306
Dominance_D	0.5779	0.2157	0.1955	0.09903	0.1707	0.1701	0.07545	0.1666	0.05828	0.07593	0.1328	0.1204	0.1823	0.3778	0.09211	0.1806	0.2778	0.212	0.2961	0.2646
Shannon_H	1,094	2,187	2,255	2,828	2,474	2,041	2,705	2,418	3,062	2,972	2,677	2,465	2,375	1.59	2,949	2,507	2,163	2,318	1,904	1,876
Equitability_J	0.4404	0.7185	0.7405	0.7892	0.6706	0.8864	0.9547	0.761	0.8834	0.8655	0.7412	0.7756	0.7052	0.64	0.8108	0.7522	0.5945	0.6419	0.5543	0.6162

cm core	981	1001	1011	1021	1051	1071	1101	1121	1151	1161	1171	1181	1191	1201	1221	1241	1251	1261	1271	1281
Taxa_S	35	34	24	27	17	22	36	32	37	40	34	37	16	39	21	30	16	31	28	29
Individuals	324	278	326	317	235	364	301	275	295	403	210	198	72	308	131	135	36	341	298	269
Dominance_D	0.3179	0.1157	0.4724	0.2822	0.3272	0.1937	0.1348	0.1168	0.09385	0.07897	0.08209	0.08198	0.2415	0.1542	0.1511	0.1132	0.09722	0.149	0.2171	0.2747
Shannon_H	2,041	2,664	1,503	1,895	1,574	2,167	2,568	2,584	2,804	2,941	2,884	3,052	1,954	2,596	2,341	2,708	2,563	2,393	2,118	2,148
Equitability_J	0.5742	0.7556	0.4729	0.5748	0.5555	0.7011	0.7165	0.7456	0.7764	0.7972	0.8177	0.8451	0.7046	0.7087	0.769	0.7962	0.9243	0.6969	0.6358	0.6378

cm core	1301	1321	1341	1351	1361	1371	1391	1401	1421	1441	1451	1471	1481	1491	1501	1521	1531	1551	1561	1581
Taxa_S	29	36	24	29	22	21	24	32	25	21	38	38	37	20	35	26	20	27	17	21
Individuals	285	279	283	278	326	262	252	325	190	221	293	200	202	99	291	280	278	296	215	267
Dominance_D	0.3655	0.1815	0.3468	0.1584	0.3226	0.4039	0.2209	0.1086	0.247	0.1861	0.08942	0.09335	0.08406	0.09479	0.1045	0.2267	0.2761	0.2797	0.2172	0.2709
Shannon_H	1,847	2.47	1,727	2,489	1,787	1,557	2,144	2,683	2,015	2.24	2,865	2,898	3,013	2,637	2,808	2,005	1,762	1,911	2,015	1,817
Equitability_J	0.5486	0.6893	0.5434	0.7391	0.5781	0.5114	0.6745	0.7742	0.6259	0.7357	0.7876	0.7968	0.8343	0.8802	0.7897	0.6155	0.5881	0.5799	0.7113	0.5967

cm core	1601	1611	1621	1631	1651	1661	1671	1701	1721	1741	1751	1761	1781	1791
Taxa_S	22	23	34	35	34	21	21	24	20	16	24	20	16	20
Individuals	267	231	363	195	333	262	304	310	238	206	246	174	174	174
Dominance_D	0.2625	0.146	0.131	0.1276	0.1503	0.1593	0.1999	0.3747	0.3288	0.163	0.1655	0.1653	0.1422	0.1968
Shannon_H	1,829	2.32	2,527	2,719	2,474	2,212	2,056	1,716	1,789	2,103	2,153	2,137	1,976	2,271
Equitability_J	0.5919	0.74	0.7167	0.7647	0.7016	0.7266	0.6752	0.5399	0.5972	0.7584	0.6773	0.7135	0.6856	0.7753

OSTRACODS

cm core	13	21	31	41	51	61	71	81	91	101	111	121	141	161	171	201	221	251	271	301
Taxa_S	2	5	5	6	5	5	7	5	6	9	3	3	4	3	5	18	3	17	6	7
Individuals	18	26	10	20	12	13	15	37	39	42	13	10	10	3	23	42	11	35	12	16
Dominance_D	0.8951	0.2722	0.4	0.26	0.2778	0.3018	0.2356	0.2432	0.499	0.2755	0.4438	0.34	0.52	0.3333	0.4442	0.2483	0.5702	0.1886	0.3056	0.3516
Shannon_H	0.2146	1,396	1,228	1,527	1,424	1,378	1,679	1,494	1,106	1,599	0.8981	1,089	0.9404	1,099	1,062	2,113	0.7595	2,272	1,474	1.45
Equitability_J	0.3095	0.8676	0.7627	0.8525	0.8849	0.8561	0.8629	0.9284	0.6174	0.7277	0.8175	0.9912	0.6784	1	0.6597	0.7311	0.6914	0.8018	0.8224	0.7452

cm core	321	351	371	391	401	411	421	451	461	471	481	491	501	541	551	561	571	591	651	671
Taxa_S	6	23	2	7	5	2	4	8	10	3	3	5	4	7	14	3	7	2	1	4
Individuals	25	65	5	10	14	3	5	24	31	3	4	25	10	10	28	3	12	2	2	6
Dominance_D	0.3984	0.1972	0.68	0.18	0.3776	0.5556	0.28	0.309	0.2508	0.3333	0.375	0.4048	0.28	0.18	0.1454	0.3333	0.2083	0.5	1	0.3333
Shannon_H	1,196	2,295	0.5004	1,834	1,253	0.6365	1,332	1,543	1.74	1,099	1.04	1,094	1,314	1,834	2.31	1,099	1,748	0.6931	0	1,242
Equitability_J	0.6676	0.732	0.7219	0.9427	0.7784	0.9183	0.961	0.7418	0.7557	1	0.9464	0.6798	0.9477	0.9427	0.8754	1	0.8984	1		0.8962

cm core	681	711	721	741	751	771	801	851	871	901	911	921	951	971	981	1001	1011	1021	1051	1071
Taxa_S	4	2	2	3	1	1	2	6	1	2	1	2	1	2	1	3	1	5	1	1
Individuals	13	3	3	4	1	1	4	11	2	4	3	7	1	5	1	5	3	9	2	1

Dominance_D	0.2899	0.5556	0.5556	0.375	1	1	0.5	0.2397	1	0.5	1	0.7551	1	0.68	1	0.36	1	0.284	1	1
Shannon_H	1,306	0.6365	0.6365	1.04	0	0	0.6931	1,594	0	0.6931	0	0.4101	0	0.5004	0	1,055	0	1,427	0	0
Equitability_J	0.9422	0.9183	0.9183	0.9464			1	0.8897		1		0.5917		0.7219		0.9602		0.8867		

cm core	1101	1121	1151	1161	1171	1181	1201	1221	1241	1251	1261	1321	1341	1351	1361	1371	1391	1401	1421	1441
Taxa_S	3	2	2	1	3	1	3	1	2	2	1	8	2	1	1	4	3	2	2	6
Individuals	4	4	5	3	6	1	9	1	4	4	1	21	3	1	2	9	3	5	4	15
Dominance_D	0.375	0.5	0.68	1	0.5	1	0.4074	1	0.625	0.625	1	0.3107	0.5556	1	1	0.4815	0.3333	0.68	0.625	0.2089
Shannon_H	1.04	0.6931	0.5004	0	0.8676	0	0.995	0	0.5623	0.5623	0	1.59	0.6365	0	0	1,003	1,099	0.5004	0.5623	1,657
Equitability_J	0.9464	1	0.7219		0.7897		0.9057		0.8113	0.8113		0.7648	0.9183			0.7233	1	0.7219	0.8113	0.9245

cm core	1451	1471	1481	1501	1521	1531	1551	1561	1581	1611	1631	1651	1661	1671	1701	1721	1741	1751	1761	1781
Taxa_S	6	4	6	1	4	5	6	5	3	7	5	2	1	1	3	4	3	4	4	2
Individuals	17	17	22	1	9	6	9	9	5	11	9	3	3	2	4	9	6	7	15	2
Dominance_D	0.2664	0.4394	0.3471	1	0.3827	0.2222	0.2099	0.2346	0.36	0.157	0.284	0.5556	1	1	0.375	0.2593	0.3889	0.3061	0.4844	0.5
Shannon_H	1,512	1,005	1,288	0	1,149	1,561	1,677	1,523	1,055	1,894	1,427	0.6365	0	0	1.04	1,369	1,011	1,277	0.9882	0.6931
Equitability_J	0.8438	0.7252	0.719		0.8289	0.9697	0.9359	0.9463	0.9602	0.9732	0.8867	0.9183			0.9464	0.9875	0.9206	0.9212	0.7128	1

cm core	1791
Taxa_S	7
Individuals	15
Dominance_D	0.2267
Shannon_H	1,714
Equitability_J	0.8809

-Deep-sea benthic response to rapid paleoclimatic changes (MIS 5 to MIS1) is analyzed.

-Stadials and interstadials are evidenced by shallow/deep benthic microhabitats.

-Intervals with deep-water formation are evidenced by particular benthic assemblages.

-Oxygen content is a main factor controlling deep-sea bottom ecosystems.